AIMS Mathematics, 10(7): 15991–16026.
DOI: 10.3934/math.2025717
Received: 01 May 2025
Revised: 19 June 2025
Accepted: 07 July 2025
Published: 16 July 2025

http://www.aimspress.com/journal/Math

Research article

Statistical inference for dependent competing-risk failures in land-based radar detection: A PHW model under generalized progressive hybrid censoring

Hanan Haj Ahmad[1,2,*], **Mohamed Aboshady**[3], **Ahmed K. Elsherif**[4] **and Dina A. Ramadan**[5]

[1] Department of Basic Science, The General Administration of Preparatory Year, King Faisal University, Hofuf, Al-Ahsa 31982, Saudi Arabia

[2] Department of Mathematics and Statistics, College of Science, King Faisal University, Al-Ahsa 31982, Saudi Arabia

[3] Department of Basic Science, Faculty of Engineering, The British University in Egypt, El Sherook City, Cairo, Egypt

[4] Department of Mathematics, Military Technical College, Cairo, Egypt

[5] Department of Mathematics, Faculty of Science, Mansoura University, Mansoura 33516, Egypt

* **Correspondence:** Email: hhajahmed@kfu.edu.sa.

Abstract: Dependent competing risks usually arise in modern reliability and survival studies, but remain under-explored because of the mathematical and computational complexity they introduce. This paper developed a flexible inferential framework for systems based on mutually dependent failure causes when the lifetimes are governed by the proportional hazard Weibull (PHW) distribution. Data were collected through the generalized progressive hybrid censoring scheme (GPHCS), which reduced test duration while preserving information with a prefixed number of failures. From a computational perspective, the maximum likelihood estimators (MLEs) were derived via numerical optimization, such as the Newton-Raphson algorithm. To incorporate prior knowledge and quantify parameter uncertainty, Bayesian estimates were produced using conjugate gamma priors and a Metropolis within Gibbs sampler. Estimator performance was assessed through an extensive Monte Carlo simulation study. Results show that MLE and Bayesian procedures were unbiased, and Bayesian credible intervals were noticeably shorter than their asymptotic counterparts. The procedure was applied to a land-based surveillance radar data set in which the target loss risks are dependent. The fitted PHW model accurately captures the dynamics of radar return signals, and posterior analyses revealed how each covariate modulates detection reliability.

Keywords: dependent competing risks; proportional hazard Weibull; generalized progressive hybrid censoring; maximum likelihood; Bayesian analysis; Monte Carlo simulation; radar signal
Mathematics Subject Classification: 60G35, 62F10, 62F15, 62N01, 62N02, 62N05

Abbreviations

PHW	proportional hazard Weibull
GPHCS	generalized progressive hybrid censoring scheme
MLE	maximum likelihood estimator
PDF	probability density function
SEL	square error loss
BCI	Bayesian credible interval
MSE	mean square error
CP	coverage probability
ACI	average credible interval
ALs	average lengths
CS	censoring schemes
KS	Kolmogorov-Smirnov

1. Introduction

In lifetime experiments, products or systems fail due to various causes throughout their life cycle. These causes interact with each other during the product's operation and are commonly referred to as the competing risk model. In real-world scenarios, the causes of failure can be independent or dependent, influenced by internal and external factors. Most discussions on the competing risk model tend to focus on independent failure causes due to their simplicity and the challenges they present in statistical analysis. For more details, refer to Fine and Lindqvist [1], Liang and Gui [2], Mahto et al. [3], Haj Ahmad et al. [4, 5], and others.

Competing risk analysis is typically used in reliability engineering and survival analysis to assess failure mechanisms where multiple risks compete to cause a system failure. On the other hand, as a result of the complexity of the internal design of components and their external operating environment, competing risks for the failure of components may be more likely to depend on each other in practice. In the literature, many authors discuss competing risk models with dependent failure causes. Some recent works of Chandra et al. [6], Samanta and Kundu [7], Tian and Gui [8], and Alqallaf and Kundu [9] have highlighted strategies for incorporating dependencies.

An important real-world context where dependent competing risks arise is radar signal detection. In such systems, environmental and operational factors can influence the radar system's ability to detect targets. Hence, radar efficiency is affected by multiple competing risks that depend on each other, for example, atmospheric conditions, electronic interference, hardware degradation, and target characteristics.

Landline surveillance radar systems are crucial in defense, air traffic control, and monitoring. Evaluating their performance requires accurate data acquisition, which is necessary to characterize the radar's capability to identify and track targets under different environmental and operational settings. For more information on radar systems and their functions, one may refer to the books of Richards [10] and Mahafza [11]. Some recent studies and applications on radar signal detection have been discussed

in the literature, such as [12, 13], among others.

This study handles the statistical inference of the unknown parameters of the proportional hazard Weibull distribution, which is utilized to model and assess radar performance with dependent competing risks. The proportional hazard Weibull distribution, denoted by PHW, is a new version of the well-known Weibull distribution that has many applications in different fields, including medical, engineering, reliability analysis, and risk assessment, due to its flexibility and effectiveness in capturing failures for various systems. The adaptability of the Weibull distribution makes it suitable for studying time-dependent system failures and the availability of events in diverse applications such as radar signal efficiency, biomedical research, and mechanical system reliability.

Unlike the basic Weibull model, the PHW model extends the analysis by including the covariates (X_i), such that the hazard function of the PHW is written as:

$$h(x) = h_0(x)x^{\beta-1},$$

where $h_0(x)$ is the hazard rate of the Weibull distribution. This enables the interaction between external factors that determine system performance, such as environmental issues and signal corruption. It also eases the evaluation of various risk groups under different conditions, allowing a more comprehensive comparison of their impact. Additionally, it improves decision-making by providing a quantitative assessment of how specific variables contribute to the overall system reliability and longevity.

Considering time and cost constraints, it is ideal to use censored sampling schemes instead of complete ones. Different censoring scenarios have been used in many research areas. Type-I censoring assumes a predetermined time, whereas Type-II censoring assumes a predetermined number of units to have failed. Many researchers have studied the progressive censoring scheme, see [14–16], which allows the removal of units at different stages of an experiment.

An essential need in reliability studies is to design a censoring scheme that balances the total test duration, the number of items evaluated, and the quality of statistical inference efficiently. Hybrid censoring, introduced initially by Epstein [17], combines the principles of Type-I and Type-II censoring and has become a standard approach in reliability testing. Numerous studies have explored this methodology in different contexts. For instance, Ebrahimi [18] and Gupta and Kundu [19] investigated hybrid censoring in the setting of exponential lifetime distributions. Lin et al. [20] applied Bayesian sampling methods to exponential data under both hybrid Type-I and Type-II schemes. [21] extended the hybrid Type-I approach to multi-sample scenarios.

Statistical models within the frameworks of hybrid censoring schemes and progressive hybrid censoring schemes have been discussed by many authors; refer to the works of Kundu [22], Kundu and Joarder [23], and Sen et al. [24] for an in-depth overview.

Due to the observed limitations in efficiency under certain hybrid censoring and progressive hybrid censoring scheme configurations, Cho et al. [25, 26] introduced a more flexible approach named the GPHCS. This method imposes a time-bound restriction on the experiment while ensuring a predetermined number of failures, contributing to more efficient statistical inference. Koley and Kundu [27] studied the GPHCS in the presence of competing risk failures. In contrast, Salem et al. [28] discussed a new scheme called the joint Type II generalized progressively hybrid censoring scheme. Dutta and Kayal presented the unified progressive hybrid censoring scheme [29] to predict and estimate failure times under Burr-III distribution. Recent applications on advanced hybrid censoring, such as in mission-oriented systems under s-dependent risks by Zhang et al. [30], further highlight the relevance

of modeling interactions and optimization in system reliability.

The GPHCS is used in this study due to its effectiveness in reducing test time and associated costs. The MLE is derived under this scheme to estimate signal detection failures caused by environmental, operational, or technical factors. Additionally, Bayesian estimation is applied to classify these failures and improve the accuracy of signal detection.

The remainder of this paper is structured in the following manner: Section 2 introduces the proposed model along with its key properties. Section 3 discusses the implementation of the MLE method, while Section 4 outlines the Bayesian inference approach. Section 5 presents a simulation study to evaluate the performance of the proposed estimation methods. In Section 6, a real-world signal dataset is analyzed to demonstrate the practical application of the model. Finally, Section 7 summarizes the main findings and concludes the study.

2. Model description and properties

This section introduces the fundamental components of the proposed modeling framework. First, we present the PHW distribution, which generalizes the classical Weibull distribution by incorporating a proportional hazard transformation, offering greater flexibility in modeling failure times. Next, we describe the GPHCS, a practical censoring strategy designed to optimize the testing process by balancing cost, time, and data informativeness. Finally, a competing risk model based on the PHW distribution is developed, providing analytical expressions for joint and marginal distributions, survival functions, and hazard rates when multiple failure causes are present.

2.1. The proportional hazard Weibull distribution

The two-parameter Weibull distribution is renowned for its adaptability and extensive use in modeling different real data, especially in reliability and engineering research, and serves as the baseline distribution for this investigation. The scale parameter α and the shape parameter β define the Weibull distribution as:

$$g(x;\alpha,\beta) = \frac{\beta}{\alpha^{\beta}} x^{\beta-1} e^{-(\frac{x}{\alpha})^{\beta}},$$

and

$$\bar{G}(x;\lambda,\alpha,\beta) = e^{-(\frac{x}{\alpha})^{\beta}},$$

representing the PDF and the survival function for the Weibull distribution, respectively. We apply the idea of the proportional hazard transform on the Weibull distribution, which is obtained using the following transformation:

$$S(x;\lambda) = [\bar{G}(x)]^{\lambda},$$

where S is the survival function of the new PHW model. For more details about the proportional hazard model, refer to Kundu [31]. This newly generated distribution has three parameters and is more flexible than the original Weibull distribution. The PDF and the reliability or survival function S for the PHW distribution are given, respectively, by:

$$f(x;\lambda,\alpha,\beta) = \frac{\lambda\beta}{\alpha^{\beta}} x^{\beta-1} e^{-\lambda(\frac{x}{\alpha})^{\beta}}, \tag{2.1}$$

and

$$S(x;\lambda,\alpha,\beta,) = e^{-\lambda(\frac{x}{\alpha})^{\beta}}. \tag{2.2}$$

The instantaneous failure rate at time x is provided by the hazard rate function $h(x)$ and can be calculated as follows:

$$h(x) = \frac{\lambda\beta}{\alpha^{\beta}}x^{\beta-1}. \tag{2.3}$$

It is important to note that while the two-parameter Weibull distribution already provides flexibility in modeling various hazard rate shapes (increasing, decreasing, or constant), the PHW distribution generalizes this by introducing a third parameter λ. This parameter acts as a proportionality constant on the hazard function, allowing for vertical scaling of the failure rate while preserving its shape. Consider the following hazard relation: $h_{PHW}(x) = \lambda h_{Weibull}(x)$. It is clear that this formulation allows the model to keep the shape of the Weibull hazard while modulating its intensity through λ, which can represent external or unobserved covariate effects. This additional degree of freedom is particularly useful in stratified or covariate-driven survival analysis, where different groups may share the same baseline hazard shape but differ in their risk levels. Hence, the PHW model offers a more adaptable framework for real-world applications requiring both shape and intensity adjustments.

The plots in Figure 1 are generated for different values of α, β, and λ, showing that the PHW distribution exhibits flexible PDF and hazard rate curves. For various combinations of these characteristics, the graphs show that the hazard rate curves can be increasing, decreasing, or constant. Figure 2 provides an extra 3D surface plot for the hazard rate function for different values of the parameters. Figure 3 visualizes how the PHW model extends the Weibull by scaling the hazard rate vertically while maintaining the underlying shape.

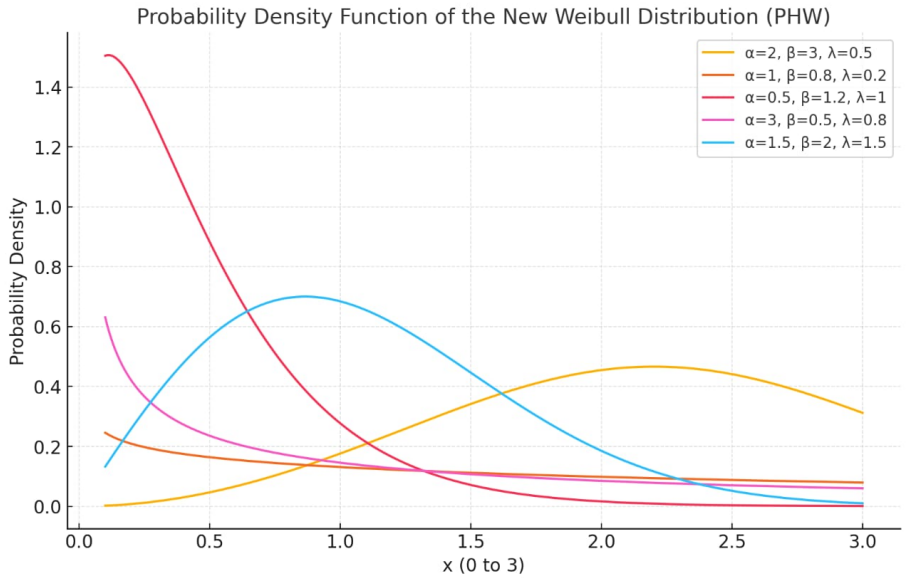

(a) PDF

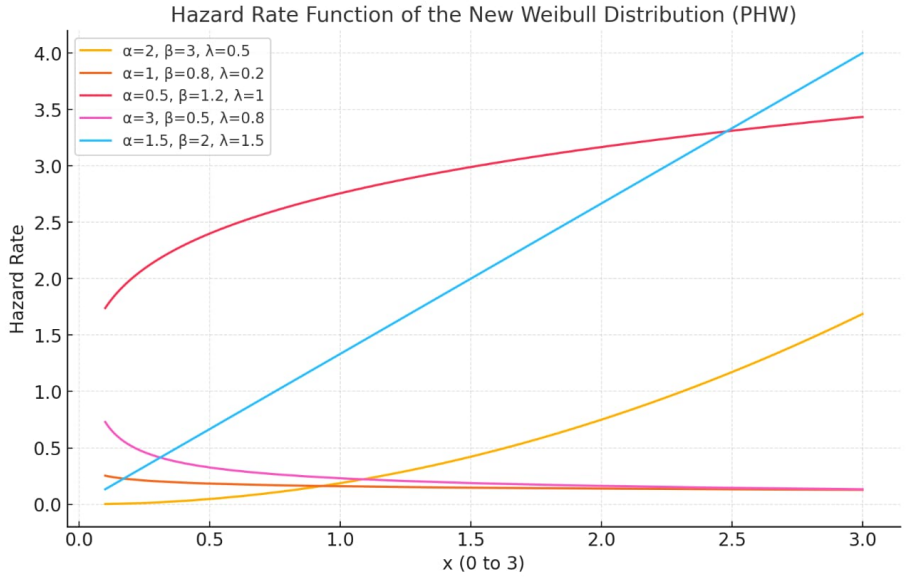

(b) Hazard Rate

Figure 1. PDF and hazard rate for the PHW with different values of α, β, and λ.

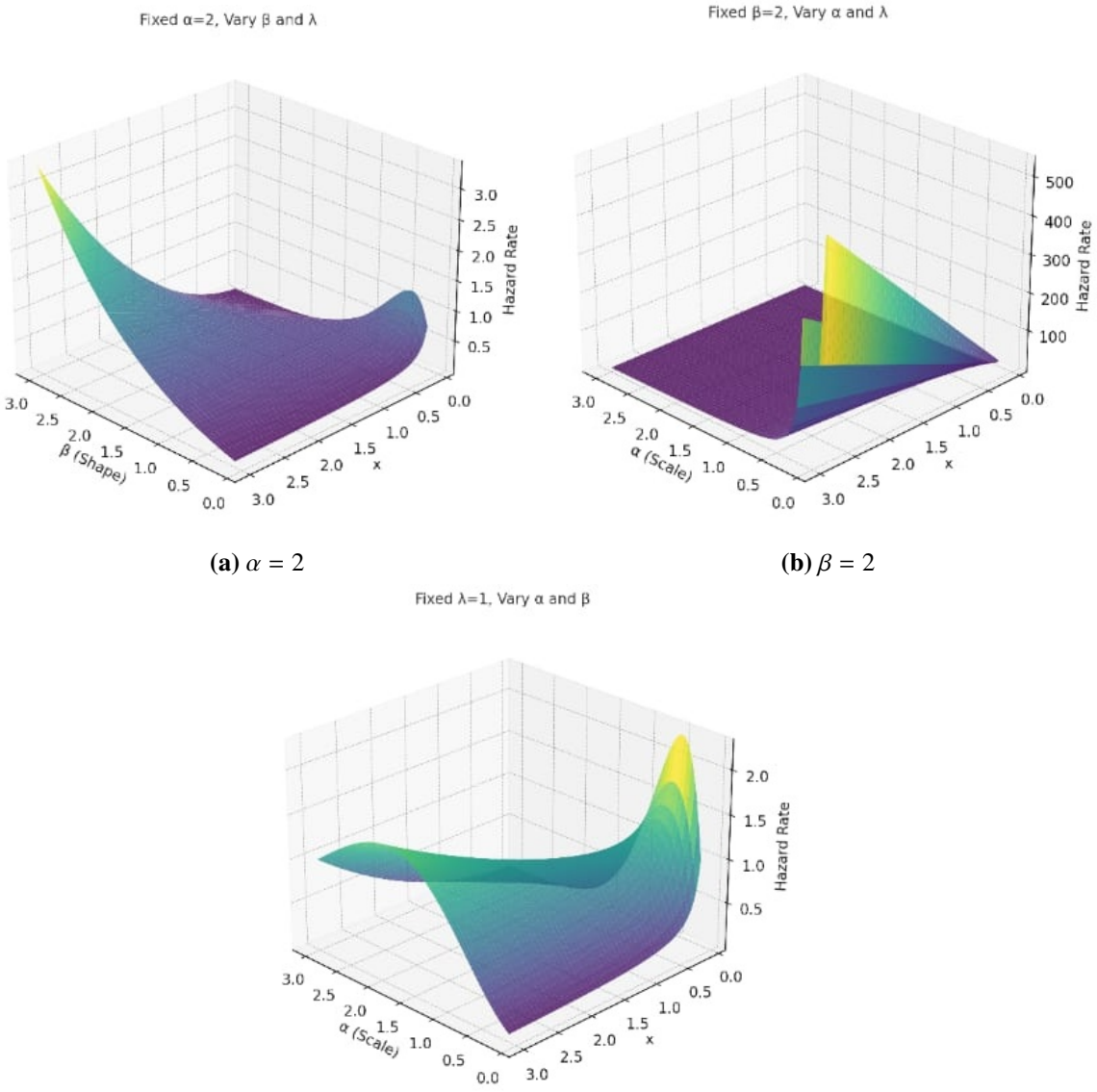

(a) $\alpha = 2$ **(b)** $\beta = 2$

(c) $\lambda = 1$

Figure 2. 3D hazard rate surface plots for different values of α, β, and λ.

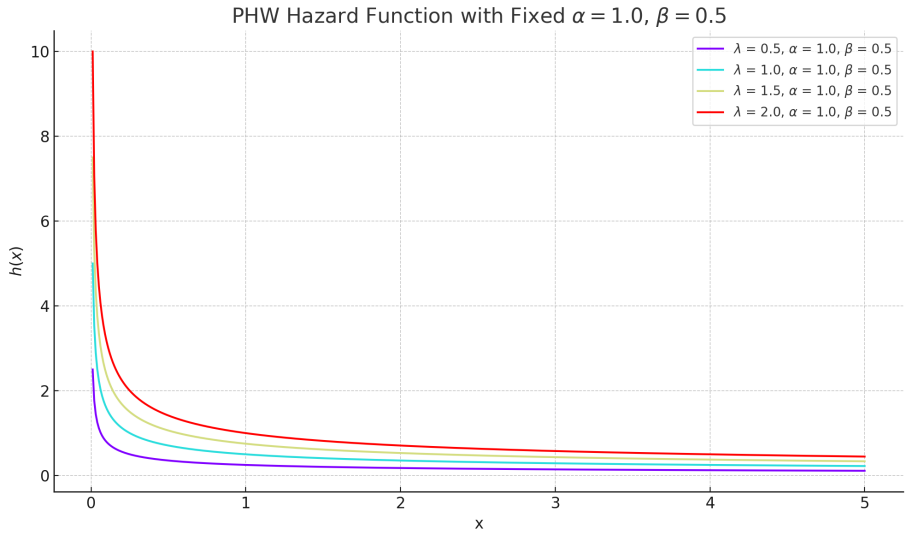

Figure 3. Comparison of the hazard rate functions for the PHW distribution with different values of λ, along with the baseline Weibull case ($\lambda = 1$).

2.2. Censoring scheme

This study considers the GPHCS, which generalizes Type-I and Type-II hybrid censoring introduced by Balakrishnan and Kundu [32]. The GPHCS defines the termination point of the experiment as a random time $T^* = \max\{X_{k:m:n}, \min\{T, X_{m:m:n}\}\}$ while testing n identical items, where m and T are prefixed numbers. For this reason, the GPHCS ensures that at least k failures are recorded. When the testing facility is contracted for a fixed duration of T time units by the experimenter and specifies that a minimum of k failures should be observed, it can employ such a censoring method. If k failures occur before time T, the experiment will continue until time T to make full use of the testing facility. If it does not occur before time T, it makes sense to keep going until the k-th failure.

The GPHCS mechanism's graphical depiction is explored in Figure 4, where $X_{j:m:n}$ represents item j's failure time. For a sample from a PHW, let $X_{1:m:n}, X_{2:m:n}, ..., X_{m:m:n}$ denote the failure times, using PDF and $S(x)$ as in Eqs 2.1 and 2.2, respectively. The expression for the likelihood function is:

$$L(\lambda, \alpha, \beta \mid \mathbf{x}) = \prod_{j=1}^{\zeta} \sum_{i=j}^{m} (1 + r_i) \prod_{i=1}^{\zeta} f\left(x_{i:\zeta:n}\right) \left[1 - F(x_{i:\zeta:n})\right]^{r_i} \left[1 - F(T)\right]^{r^*}, \tag{2.4}$$

with $\zeta = \begin{cases} k, & \text{case I} \\ d, & \text{case II} \\ m, & \text{case III} \end{cases}$, and $r^* = n - d - \sum_{i=1}^{m} r_i$.

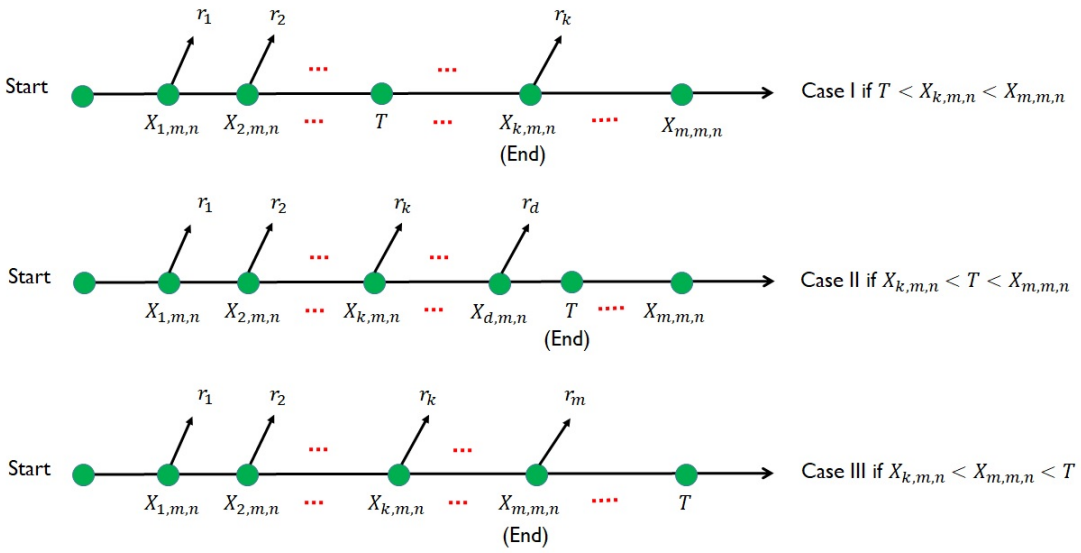

Figure 4. Graphical representation of the GPHCS scheme.

2.3. Bivariate model

To construct the bivariate PHW distribution, we consider the following latent variable representation: let U_1, U_2, U_3 be independent random variables with $U_i \sim \text{PHW}(\lambda_i, \alpha, \beta)$, $i = 1, 2, 3$, and define $X_1 = \min(U_1, U_3)$, $X_2 = \min(U_2, U_3)$. This construction induces a dependence structure between (X_1, X_2) through the common latent variable U_3. Although the marginal variables U_i are independent, the shared presence of U_3 introduces a non-trivial dependence in (X_1, X_2). The joint survival function of (X_1, X_2) is given by:

$$P(X_1 > x_1, X_2 > x_2) = \exp\left\{-\lambda_1\left(\frac{x_1}{\alpha}\right)^{\beta} - \lambda_2\left(\frac{x_2}{\alpha}\right)^{\beta} - \lambda_3\left(\frac{\max(x_1, x_2)}{\alpha}\right)^{\beta}\right\},$$

which characterizes the bivariate PHW distribution with parameters $(\lambda_1, \lambda_2, \lambda_3, \alpha, \beta)$. This formulation ensures that the marginals and minimums retain the PHW structure, as demonstrated in the following theorem.

Theorem 1. *If $(X_1, X_2) \sim PHW(\lambda_1, \lambda_2, \lambda_3, \alpha, \beta)$, then $X_1 \sim PHW(\lambda_{13}, \alpha, \beta)$, $X_2 \sim PHW(\lambda_{23}, \alpha, \beta)$, and $min(X_1, X_2) \sim PHW(\lambda_{123}, \alpha, \beta)$.*

Theorem 2. *The joint survival function is given by the following expression:*

$$S_{(X_1,X_2)}(x_1, x_2) = \begin{cases} S(x_1; \lambda_1, \alpha, \beta)S(x_2; \lambda_{23}, \alpha, \beta), & x_1 < x_2, \\ S(x_1; \lambda_{13}, \alpha, \beta)S(x_2; \lambda_2, \alpha, \beta), & x_1 > x_2, \\ S(x; \lambda_{123}, \alpha, \beta), & x_1 = x_2 = x. \end{cases} \tag{2.5}$$

Theorem 3. *The joint PDF of (X_1, X_2) can be written as*

$$f_{(X_1,X_2)}(x_1, x_2) = \begin{cases} f_1(x_1, x_2) = f(x_1; \lambda_1, \alpha, \beta)f(x_2; \lambda_{23}, \alpha, \beta), & x_1 < x_2, \\ f_2(x_1, x_2) = f(x_1; \lambda_{13}, \alpha, \beta)f(x_2; \lambda_2, \alpha, \beta), & x_1 > x_2, \\ f_3(x) = \frac{\lambda_3}{\lambda_{123}} f(x; \lambda_{123}, \alpha, \beta), & x_1 = x_2 = x. \end{cases} \tag{2.6}$$

Appendices 1–3 contain the complete proofs of Theorems 1–3, respectively.

3. Maximum likelihood inference

This section uses the MLE method to observe point and interval estimators of the PHW parameters under dependent competing risks, and data are obtained from the GPHCS. The MLE is well known for its desirable asymptotic properties, such as invariance, consistency, asymptotic normality, and efficiency (large sample size). These properties make it the best choice for estimation and statistical inference. See Casella and Berger [33] and Lawless [34] as main references. It is also noticed that the MLE is adaptable with complex censoring schemes such as the GPHCS, see [25] and [27].

Here, we assume no restrictions for the competing risks parameters.

3.1. Point estimation

The joint likelihood function under the GPHCS is given by

$$L \propto \begin{cases} \prod_{i=1}^{k} \left[f_{(X_1,X_2)}(y_i,y_i)\right]^{\delta_{i0}} \left[-\left.\frac{\partial S_{(X_1,X_2)}(x_1,x_2)}{\partial x_1}\right|_{(y_i,y_i)}\right]^{\delta_{i1}} \\ \left[-\left.\frac{\partial S_{(X_1,X_2)}(x_1,x_2)}{\partial x_2}\right|_{(y_i,y_i)}\right]^{\delta_{i2}} \left[S_{(X_1,X_2)}(y_i,y_i)\right]^{r_i}, & \text{case I} \\ \prod_{i=1}^{d} \left[f_{(X_1,X_2)}(y_i,y_i)\right]^{\delta_{i0}} \left[-\left.\frac{\partial S_{(X_1,X_2)}(x_1,x_2)}{\partial x_1}\right|_{(y_i,y_i)}\right]^{\delta_{i1}} \\ \left[-\left.\frac{\partial S_{(X_1,X_2)}(x_1,x_2)}{\partial x_2}\right|_{(y_i,y_i)}\right]^{\delta_{i2}} \left[S_{(X_1,X_2)}(y_i,y_i)\right]^{r_i} \left[S_{(X_1,X_2)}(T,T)\right]^{r^*_{d+1}}, & \text{case II} \\ \prod_{i=1}^{m} \left[f_{(X_1,X_2)}(y_i,y_i)\right]^{\delta_{i0}} \left[-\left.\frac{\partial S_{(X_1,X_2)}(x_1,x_2)}{\partial x_1}\right|_{(y_i,y_i)}\right]^{\delta_{i1}} \\ \left[-\left.\frac{\partial S_{(X_1,X_2)}(x_1,x_2)}{\partial x_2}\right|_{(y_i,y_i)}\right]^{\delta_{i2}} \left[S_{(X_1,X_2)}(y_i,y_i)\right]^{r_i}, & \text{case III} \end{cases}$$

where $r^*_{d+1} = n - \sum_{i=1}^{d}(r_i+1)$ and $r_k = n - \sum_{i=1}^{k-1}(r_i+1) - 1$, and $\delta_{ij} = 1$, if $\delta_i = j$, which refers to a binary indicator stating whether the i^{th} failure occurred under cause $j = 1, 2$. Hence, the likelihood functions $L_1,\ L_2,$ and L_3 based on the observed data set in the three cases will be given as

$$L_1(\lambda_1,\lambda_2,\lambda_3,\alpha,\beta) = \frac{\lambda_1^{\eta_1}\lambda_2^{\eta_2}\lambda_3^{\eta_3}\beta^k}{\alpha^{k\beta}} \prod_{i=1}^{k} y_i^{\beta-1} e^{-\lambda_{123}\sum_{i=1}^{k}(1+r_i)(\frac{y_i}{\alpha})^{\beta}},$$

$$L_2(\lambda_1,\lambda_2,\lambda_3,\alpha,\beta) = \frac{\lambda_1^{\eta_1}\lambda_2^{\eta_2}\lambda_3^{\eta_3}\beta^d}{\alpha^{d\beta}} \prod_{i=1}^{d} y_i^{\beta-1} e^{-\lambda_{123}\left[\sum_{i=1}^{d}(1+r_i)(\frac{y_i}{\alpha})^{\beta} + r^*_{d+1}(\frac{T}{\alpha})^{\beta}\right]},$$

$$L_3(\lambda_1,\lambda_2,\lambda_3,\alpha,\beta) = \frac{\lambda_1^{\eta_1}\lambda_2^{\eta_2}\lambda_3^{\eta_3}\beta^m}{\alpha^{m\beta}} \prod_{i=1}^{m} y_i^{\beta-1} e^{-\lambda_{123}\sum_{i=1}^{m}(1+r_i)(\frac{y_i}{\alpha})^{\beta}},$$

where $\eta_1 = \sum_{i=1}^{d^*} \delta_{i1},\ \eta_2 = \sum_{i=1}^{d^*} \delta_{i2},\ \eta_1 = \sum_{i=1}^{d^*} \delta_{i3},\ \delta_{i1} + \delta_{i2} + \delta_{i3} = 1.$

The likelihood function can be combined as:

$$L(\lambda_1, \lambda_2, \lambda_3, \alpha, \beta) = \frac{\lambda_1^{\eta_1} \lambda_2^{\eta_2} \lambda_3^{\eta_3} \beta^{\zeta}}{\alpha^{\zeta\beta}} \prod_{i=1}^{\zeta} y_i^{\beta-1} e^{-\lambda_{123} z_1(\alpha,\beta)}, \tag{3.1}$$

where

$$z_1(\alpha,\beta) = \begin{cases} \sum_{i=1}^{k} (1 + r_i) \left(\frac{y_i}{\alpha}\right)^{\beta}, & \text{case I,} \\ \sum_{i=1}^{d} (1 + r_i) \left(\frac{y_i}{\alpha}\right)^{\beta} + r_{d+1}^* \left(\frac{T}{\alpha}\right)^{\beta}, & \text{case II,} \\ \sum_{i=1}^{m} (1 + r_i) \left(\frac{y_i}{\alpha}\right)^{\beta}, & \text{case III.} \end{cases} \tag{3.2}$$

Therefore, the corresponding log-likelihood function is observed as:

$$\ln L = \sum_{j=1}^{3} \eta_j \ln(\lambda_j) + \zeta(\ln\beta - \beta \ln\alpha) + (\beta - 1) \sum_{i=1}^{\zeta} \ln y_i - \lambda_{123} z_1(\alpha,\beta). \tag{3.3}$$

The MLE $\hat{\lambda}_j$ of parameters λ_j can be found using the following equation through calculating the derivative of $\ln L$ with respect to λ_j and setting it to zero:

$$\frac{\partial \ln L}{\partial \lambda_j} = \frac{\eta_j}{\lambda_j} - z_1(\alpha,\beta) = 0, \tag{3.4}$$

leading to $\hat{\lambda}_j = \frac{\eta_j}{z_1(\alpha,\beta)}$.

Similarly, differentiating with respect to the parameters α and β, we have:

$$\frac{\partial \ln L}{\partial \alpha} = \frac{\zeta\beta}{\alpha} - \lambda_{123} z_2(\alpha,\beta), \tag{3.5}$$

and

$$\frac{\partial \ln L}{\partial \beta} = \frac{\zeta}{\beta} - \zeta \ln\alpha + \sum_{i=1}^{\zeta} \ln y_i - \lambda_{123} z_3(\alpha,\beta), \tag{3.6}$$

where

$$z_2(\alpha,\beta) = \begin{cases} -\sum_{i=1}^{k} (1 + r_i) \beta y_i^{\beta} \alpha^{-\beta-1}, & \text{case I,} \\ -\sum_{i=1}^{d} (1 + r_i) \beta y_i^{\beta} \alpha^{-\beta-1} - \beta r_{d+1}^* T^{\beta} \alpha^{-\beta-1}, & \text{case II,} \\ -\sum_{i=1}^{m} (1 + r_i) \beta y_i^{\beta} \alpha^{-\beta-1}, & \text{case III,} \end{cases} \tag{3.7}$$

and

$$z_3(\alpha,\beta)=\begin{cases}\displaystyle\sum_{i=1}^{k}(1+r_i)\left(\frac{y_i}{\alpha}\right)^{\beta}\ln\left(\frac{y_i}{\alpha}\right), & \text{case I},\\ \displaystyle\sum_{i=1}^{d}(1+r_i)\left(\frac{y_i}{\alpha}\right)^{\beta}\ln\left(\frac{y_i}{\alpha}\right)+r^{*}_{d+1}\left(\frac{T}{\alpha}\right)^{\beta}\ln\left(\frac{T}{\alpha}\right), & \text{case II},\\ \displaystyle\sum_{i=1}^{m}(1+r_i)\left(\frac{y_i}{\alpha}\right)^{\beta}\ln\left(\frac{y_i}{\alpha}\right), & \text{case III}.\end{cases} \tag{3.8}$$

3.2. Confidence interval

In this section, we derive approximate confidence intervals for the unknown parameters of the PHW distribution based on the asymptotic properties of the MLE. Given the complexity involved in computing the expected Fisher information, we utilize the observed Fisher information matrix instead to simplify the calculations, which is expressed as follows:

$$\hat{I}(\lambda_i,\alpha,\beta)=\begin{pmatrix}\frac{\eta_1}{\lambda_1^2} & 0 & 0 & z_2 & z_3\\ 0 & \frac{\eta_2}{\lambda_2^2} & 0 & z_2 & z_3\\ 0 & 0 & \frac{\eta_3}{\lambda_3^2} & z_2 & z_3\\ z_2 & z_2 & z_2 & \frac{\zeta\beta}{\alpha^2}+\lambda_{123}z_2^{\prime\alpha} & \frac{\zeta}{\alpha}+\lambda_{123}z_2^{\prime\beta}\\ z_3 & z_3 & z_3 & \frac{\zeta}{\alpha}+\lambda_{123}z_3^{\prime\beta} & \frac{\zeta}{\beta^2}+\lambda_{123}z_3^{\prime\beta}\end{pmatrix}, \tag{3.9}$$

such that $z_2^{\prime\alpha}=\frac{\partial z_2}{\partial\alpha}$, $z_2^{\prime\beta}=\frac{\partial z_2}{\partial\beta}$, and $z_3^{\prime\beta}=\frac{\partial z_3}{\partial\beta}$, where their values are given as:

$$z_2^{\prime\beta}(\alpha,\beta)=\begin{cases}-\displaystyle\sum_{i=1}^{k}(1+r_i)[y_i^{\beta}\alpha^{-\beta-1}+\beta y_i^{\beta}\alpha^{-\beta-1}\ln y_i-\beta y_i^{\beta}\alpha^{-\beta-1}\ln\alpha], & \text{case I},\\ -\displaystyle\sum_{i=1}^{d}(1+r_i)[y_i^{\beta}\alpha^{-\beta-1}+\beta y_i^{\beta}\alpha^{-\beta-1}\ln y_i-\beta y_i^{\beta}\alpha^{-\beta-1}\ln\alpha]\\ -r^{*}_{d+1}[T^{\beta}\alpha^{-\beta-1}+\beta T^{\beta}\alpha^{-\beta-1}\ln T-\beta T^{\beta}\alpha^{-\beta-1}\ln\alpha], & \text{case II},\\ -\displaystyle\sum_{i=1}^{m}(1+r_i)[y_i^{\beta}\alpha^{-\beta-1}+\beta y_i^{\beta}\alpha^{-\beta-1}\ln y_i-\beta y_i^{\beta}\alpha^{-\beta-1}\ln\alpha], & \text{case III},\end{cases} \tag{3.10}$$

$$z_2^{\prime\alpha}(\alpha,\beta)=\begin{cases}\displaystyle\sum_{i=1}^{k}(1+r_i)\beta(\beta+1)y_i^{\beta}\alpha^{-\beta-2}, & \text{case I},\\ \displaystyle\sum_{i=1}^{d}(1+r_i)\beta(\beta+1)y_i^{\beta}\alpha^{-\beta-2}\\ +\beta(\beta+1)r^{*}_{d+1}T^{\beta}\alpha^{-\beta-2}, & \text{case II},\\ \displaystyle\sum_{i=1}^{m}(1+r_i)\beta(\beta+1)y_i^{\beta}\alpha^{-\beta-2}, & \text{case III},\end{cases} \tag{3.11}$$

$$z_3'^{\beta}(\alpha,\beta) = \begin{cases} \sum_{i=1}^{k}(1+r_i)\left(\frac{y_i}{\alpha}\right)^{\beta}\left[\ln\left(\frac{y_i}{\alpha}\right)\right]^2, & \text{case I,} \\ \sum_{i=1}^{d}(1+r_i)\left(\frac{y_i}{\alpha}\right)^{\beta}\left[\ln\left(\frac{y_i}{\alpha}\right)\right]^2 + r^*_{d+1}\left(\frac{T}{\alpha}\right)^{\beta}\left[\ln\left(\frac{T}{\alpha}\right)\right]^2, & \text{case II,} \\ \sum_{i=1}^{m}(1+r_i)\left(\frac{y_i}{\alpha}\right)^{\beta}\left[\ln\left(\frac{y_i}{\alpha}\right)\right]^2, & \text{case III.} \end{cases} \tag{3.12}$$

Now using the asymptotic property of the MLE, and assuming the vector of parameters $\boldsymbol{\phi} = \{\lambda_1, \lambda_2, \lambda_3, \alpha, \beta\}$, the following holds:

$$\hat{\boldsymbol{\phi}} - \boldsymbol{\phi} \to N(0, I^{-1}(\hat{\boldsymbol{\phi}})),$$

where

$$I^{-1}(\hat{\boldsymbol{\phi}}) = \begin{pmatrix} Var(\hat{\lambda}_1) & Cov(\hat{\lambda}_1,\hat{\lambda}_2) & Cov(\hat{\lambda}_1,\hat{\lambda}_3) & Cov(\hat{\lambda}_1,\hat{\alpha}) & Cov(\hat{\lambda}_1,\hat{\beta}) \\ Cov(\hat{\lambda}_1,\hat{\lambda}_2) & Var(\hat{\lambda}_2) & Cov(\hat{\lambda}_2,\hat{\lambda}_3) & Cov(\hat{\lambda}_2,\hat{\alpha}) & Cov(\hat{\lambda}_2,\hat{\beta}) \\ Cov(\hat{\lambda}_1,\hat{\lambda}_3) & Cov(\hat{\lambda}_2,\hat{\lambda}_3) & Var(\hat{\lambda}_3) & Cov(\hat{\lambda}_3,\hat{\alpha}) & Cov(\hat{\lambda}_3,\hat{\beta}) \\ Cov(\hat{\lambda}_1,\hat{\alpha}) & Cov(\hat{\lambda}_2,\hat{\alpha}) & Cov(\hat{\lambda}_3,\hat{\alpha}) & Var(\hat{\alpha}) & Cov(\hat{\alpha},\hat{\beta}) \\ Cov(\hat{\lambda}_1,\hat{\beta}) & Cov(\hat{\lambda}_2,\hat{\beta}) & Cov(\hat{\lambda}_3,\hat{\beta}) & Cov(\hat{\alpha},\hat{\beta}) & Var(\hat{\beta}) \end{pmatrix}. \tag{3.13}$$

Let $0 < \psi < 1$, and then a $(1-\psi)100\%$ confidence interval for $\boldsymbol{\phi}$ is given by:

$$(\hat{\boldsymbol{\phi}} \pm w_{\psi/2}\sqrt{Var(\hat{\boldsymbol{\phi}})}),$$

where w_ψ refers to the upper 100ψ percentile in the standard normal table.

4. Bayesian estimation

In Bayesian inference, parameter estimation involves the combination of prior knowledge with the observed data to form updated beliefs about the unknown quantities, namely λ_1, λ_2, λ_3, α, and β. The prior distribution serves as a mathematical representation of the experimenter's assumptions about these parameters before data observation. To reflect this prior, hyperparameters a_i and b_i, for $i = 1, \ldots, 5$, are selected accordingly. In this framework, an informative gamma distribution is adopted as the prior due to its desirable analytical properties and its suitability for modeling positive, continuous-valued parameters. It is mathematically convenient, conceptually attractive, and computationally friendly. The gamma prior is flexible, and its conjugacy properties with many likelihood functions make it a powerful tool for representing prior knowledge and updating beliefs in light of new data. This choice is especially appropriate for modeling the rate or shape parameters of certain distributions. The prior formulation can be mathematically expressed as:

$$\begin{aligned} &\pi_i(\lambda_i) \propto \lambda_i^{a_i-1}e^{-b_i\lambda_i}, && \lambda_i > 0, a_i > 0, b_i > 0,\ i = 1,2,3, \\ &\pi_4(\alpha) \propto \alpha^{a_4-1}e^{-b_4\alpha}, && \alpha > 0, a_4 > 0, b_4 > 0, \\ &\pi_5(\beta) \propto \beta^{a_5-1}e^{-b_5\beta}, && \beta > 0, a_5 > 0, b_5 > 0. \end{aligned} \tag{4.1}$$

The joint prior distribution can be written as

$$\pi(\lambda_1, \lambda_2, \lambda_3, \alpha, \beta) \propto \lambda_1^{a_1-1}\lambda_2^{a_2-1}\lambda_3^{a_3-1}\alpha^{a_4-1}\beta^{a_5-1}e^{-(b_1\lambda_1+b_2\lambda_2+b_3\lambda_3+b_4\alpha+b_5\beta)}.$$

The expression for the joint posterior density is given by:

$$\begin{aligned}\pi^*(\boldsymbol{\phi} \mid \text{data}) &\propto \pi(\boldsymbol{\phi})L(\boldsymbol{\phi}) \\ &= \frac{\lambda_1^{\eta_1+a_1-1}\lambda_2^{\eta_2+a_2-1}\lambda_3^{\eta_3+a_3-1}\beta^{\zeta+a_5-1}}{\alpha^{\zeta\beta-a_4+1}}e^{-(b_1\lambda_1+b_2\lambda_2+b_3\lambda_3+b_4\alpha+b_5\beta)}\prod_{i=1}^{\zeta}y_i^{\beta-1}e^{-\lambda_{123}z_1(\alpha,\beta)}. \end{aligned} \tag{4.2}$$

The conditional posterior densities of $\boldsymbol{\phi}$ and the data can be provided as

$$\pi_1^*(\lambda_1 \mid \lambda_2, \lambda_3, \alpha, \beta; \text{data}) \propto \lambda_1^{\eta_1+a_1-1}e^{-b_1\lambda_1}e^{-\lambda_{123}z_1(\alpha,\beta)}, \tag{4.3}$$

$$\pi_2^*(\lambda_2 \mid \lambda_1, \lambda_3, \alpha, \beta; \text{data}) \propto \lambda_2^{\eta_2+a_2-1}e^{-b_2\lambda_2}e^{-\lambda_{123}z_1(\alpha,\beta)}, \tag{4.4}$$

$$\pi_3^*(\lambda_3 \mid \lambda_1, \lambda_2, \alpha, \beta; \text{data}) \propto \lambda_3^{\eta_3+a_3-1}e^{-b_3\lambda_3}e^{-\lambda_{123}z_1(\alpha,\beta)}, \tag{4.5}$$

$$\pi_4^*(\alpha \mid \lambda_1, \lambda_2, \lambda_3, \beta; \text{data}) \propto \alpha^{-\zeta\beta+a_4-1}e^{-b_4\alpha}e^{-\lambda_{123}z_1(\alpha,\beta)}, \tag{4.6}$$

and

$$\pi_5^*(\beta \mid \lambda_1, \lambda_2, \lambda_3, \alpha; \text{data}) \propto \beta^{\zeta+a_5-1}e^{-b_5\beta}\prod_{i=1}^{\zeta}y_i^{\beta-1}e^{-\lambda_{123}z_1(\alpha,\beta)}. \tag{4.7}$$

The definition of the SEL is $L\left(\hat{\boldsymbol{\phi}}-\boldsymbol{\phi}\right) = \left(\hat{\boldsymbol{\phi}}-\boldsymbol{\phi}\right)^2$, where $\boldsymbol{\phi} = (\lambda_1, \lambda_2, \lambda_3, \alpha, \beta)$ and $d\boldsymbol{\phi} = (d\lambda_1, d\lambda_2, d\lambda_3, d\alpha, d\beta)$. $\boldsymbol{D(\phi)}$ refers to the domain of the parameters $\lambda_1, \lambda_2, \lambda_3, \alpha, \beta$ which was defined to be $(0, \infty)$. This loss function is symmetric; that is, it gives equal weight to both over-and underestimation. Overestimation can often be worse than underestimation in real-world experiments, or vice versa.

The Bayes estimation of $\lambda_1, \lambda_2, \lambda_3, \alpha,$ and β are obtained, respectively, as:

$$\begin{aligned}\hat{\lambda}_{1SB} &= E\left(\lambda_1 \mid \lambda_2, \lambda_3, \beta, \alpha, \text{ data}\right) \\ &= K^{-1}\int_{\boldsymbol{D(\phi)}}\lambda_1^{\eta_1+a_1-1}e^{-b_1\lambda_1}e^{-\lambda_{123}z_1(\alpha,\beta)}d\boldsymbol{\phi},\end{aligned}$$

$$\begin{aligned}\hat{\lambda}_{2SB} &= E\left(\lambda_2 \mid \lambda_1, \lambda_3, \beta, \alpha, \text{ data}\right) \\ &= K^{-1}\int_{\boldsymbol{D(\phi)}}\lambda_2^{\eta_2+a_2-1}e^{-b_2\lambda_2}e^{-\lambda_{123}z_1(\alpha,\beta)}d\boldsymbol{\phi},\end{aligned}$$

$$\hat{\lambda}_{3SB} = E\left(\lambda_3 \mid \lambda_1, \lambda_2, \beta, \alpha, \text{ data}\right)$$

$$= K^{-1} \int_{\boldsymbol{D}(\boldsymbol{\phi})} \lambda_3^{\eta_3+a_3-1} e^{-b_3\lambda_3} e^{-\lambda_{123} z_1(\alpha,\beta)} d\boldsymbol{\phi},$$

$$\begin{aligned}\hat{\alpha}_{SB} &= E\left(\alpha \mid \lambda_1, \lambda_2, \lambda_3, \beta, \text{ data}\right) \\ &= K^{-1} \int_{\boldsymbol{D}(\boldsymbol{\phi})} \alpha^{-\zeta\beta+a_4-1} e^{-b_4\alpha} e^{-\lambda_{123} z_1(\alpha,\beta)} d\boldsymbol{\phi},\end{aligned}$$

and

$$\begin{aligned}\hat{\beta}_{SB} &= E\left(\beta \mid \lambda_1, \lambda_2, \lambda_3, \alpha, \text{ data}\right) \\ &= K^{-1} \int_{\boldsymbol{D}(\boldsymbol{\phi})} \beta^{\zeta+a_5-1} e^{-b_5\beta} \prod_{i=1}^{\zeta} y_i^{\beta-1} e^{-\lambda_{123} z_1(\alpha,\beta)} d\boldsymbol{\phi},\end{aligned}$$

where

$$\begin{aligned}K &= \int_{\boldsymbol{D}(\boldsymbol{\phi})} \pi\left(\lambda_1, \lambda_2, \lambda_3, \alpha, \beta\right) \; L(\lambda_1, \lambda_2, \lambda_3, \alpha, \beta \mid \text{data}) \, d\boldsymbol{\phi} \\ &= \int_{\boldsymbol{D}(\boldsymbol{\phi})} \frac{\lambda_1^{\eta_1+a_1-1} \lambda_2^{\eta_2+a_2-1} \lambda_3^{\eta_3+a_3-1} \beta^{\zeta+a_5-1}}{\alpha^{\zeta\beta-a_4+1}} e^{-(b_1\lambda_1+b_2\lambda_2+b_3\lambda_3+b_4\alpha+b_5\beta)} \prod_{i=1}^{\zeta} y_i^{\beta-1} e^{-\lambda_{123} z_1(\alpha,\beta)} d\boldsymbol{\phi}.\end{aligned}$$

Consequently, under the SEL, the Bayes estimate of any function with variables $\lambda_1, \lambda_2, \lambda_3, \alpha$, and β, such as $g(\lambda_1, \lambda_2, \lambda_3, \alpha, \beta)$, may be found as follows:

$$\hat{g}_{BS}\left(\boldsymbol{\phi} \mid \text{data}\right) = E_{\boldsymbol{\phi}|\text{data}}\left(g\left(\boldsymbol{\phi}\right)\right), \tag{4.8}$$

where

$$E_{\boldsymbol{\phi}|\text{data}}\left(g\left(\boldsymbol{\phi}\right)\right) = \frac{\int_{\boldsymbol{D}(\boldsymbol{\phi})} g\left(\boldsymbol{\phi}\right) \; \pi_1\left(\lambda_1\right) \pi_2\left(\lambda_2\right) \pi_3\left(\lambda_3\right) \pi_4\left(\alpha\right) \; \pi_5\left(\beta\right) \; L(\boldsymbol{\phi} \mid \text{data}) d\boldsymbol{\phi}}{\int_{\boldsymbol{D}(\boldsymbol{\phi})} \pi_1\left(\lambda_1\right) \pi_2\left(\lambda_2\right) \pi_3\left(\lambda_3\right) \pi_4\left(\alpha\right) \; \pi_5\left(\beta\right) \; L(\boldsymbol{\phi} \mid \text{data}) \, d\boldsymbol{\phi}}. \tag{4.9}$$

Obtaining Bayesian estimates for the parameters $\lambda_1, \lambda_2, \lambda_3, \alpha$, and β within the PHW framework is analytically intractable, particularly under the constraints of the GPHCS. To overcome this issue, we adopt the MCMC technique, which serves as an efficient numerical tool for approximating posterior distributions when explicit analytical computations are not feasible (see Eq (4.2)). The Metropolis-Hasting method through Gibbs sampling is the best option because it is evident that the conditional posteriors of $\lambda_1, \lambda_2, \lambda_3, \alpha$, and β in Eqs (4.3)–(4.7) are not available in normal forms. The Metropolis-Hasting sampler is essential to the MCMC technique's implementation. The way the MCMC method operates is by producing a series of samples that roughly correspond to the parameters' posterior

distribution. A Markov chain that converges to the intended distribution over time is simulated to create this sequence. We may estimate posterior statistics, like the mean, which are Bayesian estimates for $\lambda_1, \lambda_2, \lambda_3, \alpha$, and β, by collecting samples from this chain.

MCMC relies heavily on Metropolis-in-Gibbs samplers and Gibbs sampling. For example, Metropolis et al. [35] and Hastings [36] discussed how Gibbs sampling is especially helpful when we take samples straight from the conditional distributions for every parameter, given the others. By sequentially updating the parameters in each Gibbs sampling iteration using these conditional distributions, the sampler can effectively explore the parameter space. The algorithm structure can be further explained by consulting [4].

The Metropolis-Hastings algorithm is necessary for the creation of the BCI. As a result, the choice of variance is crucial; for further information, see Ntzoufras [37]. The Fisher information criteria would be an additional option for variance. For more details, see Robert and Casella [38] and Chib and Greenberg [39].

5. Simulation analysis

This section analyzes the different estimators obtained from the two estimation methods, MLE and Bayesian, under the GPHCS using a comprehensive Monte Carlo simulation. Data in this work are collected for three CS, various sample sizes (n, m), and experimental parameters T and k. Additionally, the point estimators of the PHW distribution parameters are assessed using MSEs to investigate the performance of various estimates, while interval estimates are analyzed using ALs, ACIs, and CPs. Arbitrary values for $(\alpha, \beta, \lambda_1, \lambda_2, \lambda_3)$ are selected as the true values in this simulation work as $(2, 5, 4, 3, 1)$. Consideration is given to $(n, m) = (50, 40)$ and $(80, 65)$ in this simulation, where in the case $(n, m) = (50, 40)$, the values for k are 25, 30, and 35, and in the case where $(n, m) = (80, 75)$, they are 30, 45, and 55. In addition, two values are considered for T as 0.5 and 0.8. Bayes estimates for the PHW distribution are calculated under the informative prior using the hyperparameters $a_1 = 10$, $a_2 = 15$, $a_3 = 140$, $a_4 = 200$, $a_5 = 0.0005$, $b_1 = 0.3$, $b_2 = 0.05$, $b_3 = 0.05$, $b_4 = 0.0001$, $b_5 = 18$. The following is how the three different censoring schemes are used:

Scheme I: $r_i = 2,\ i = 2 : 5$, and $r_j = 0,\ j = 1 : m,\ j \neq i$.
Scheme II: $r_i = 2,\ i = 12 : 15$, and $r_j = 0,\ j = 1 : m,\ j \neq i$.
Scheme III: $r_i = 2,\ i = 22 : 25$, and $r_j = 0,\ j = 1 : m,\ j \neq i$.

Different criteria combinations are obtained based on 1000 repetitions, and the simulation results for various approaches are provided, with the values of the MSE and CP shown in parentheses.

- Table 1 shows that although the Bayesian estimates typically have slightly larger values, the MLEs and Bayesian estimates for α are generally close. Different censoring schemes (CS I, II, and III) have varying MSEs; CS III frequently has higher MSEs, which suggests less precision. Lower MSEs, which indicate better estimation accuracy, are typically obtained from larger sample sizes ($n = 80$, for example).
- In Table 2, the CPs are primarily above 93%, indicating high coverage and the ACIs are comparatively narrow, indicating accurate estimations. Some CPs, however, differ marginally from the 95% level, which might be because of sample sizes or censoring schemes. Although the

differences are not constant, Bayesian approaches sometimes provide superior coverage.

- For β in Table 3, the Bayesian estimates and MLEs never vary, indicating that the two approaches converge to the same point estimates for this parameter. MSEs differ between censoring schemes; CS II frequently has larger MSEs, which suggests less accuracy. In general, larger sample sizes ($n = 80$, for example) result in reduced MSEs, indicating higher estimation accuracy.
- The extremely narrow ACIs (0.0004–0.0012, for example) in Table 4 suggest very accurate estimations. There are occasional variances, especially for smaller sample sizes, but generally speaking, the CPs are near or above the nominal 95% level. Similar ACI lengths and CPs show that estimates from the MLE and Bayesian approaches are consistent.
- Across all censoring schemes, the Bayesian estimates for λ_1 in Table 5 are consistently just slightly higher than the MLEs, indicating a systematic increase in the Bayesian approach. The MSEs differ significantly, and CS III frequently shows the largest errors (e.g., 5.7337 for MLE at $n = 50, m = 40, T = 0.5, k = 25$), suggesting that this scheme is less precise. Although there are some exceptions (such as the extreme outlier 7.7363 for Bayesian in CS III), larger sample sizes ($n = 80$) typically result in lower MSEs. MSEs can occasionally increase with longer censoring times ($T = 0.8$) (for example, from 1.2136 to 4.8968 for CS I with MLE at $k = 25$), indicating sensitivity to the censoring scheme.
- Due to tighter uncertainty estimates, Bayesian intervals in Table 6 are noticeably smaller than the MLE intervals (e.g., 0.3401 vs. 0.4418 for CS I at $n = 50, T = 0.5, k = 25$). However, some small intervals (such as 0.1383 for CS II Bayesian) would be worth investigating because they might be under-covered. Although some decreases in CPs (such as 0.9342 for MLE in CS I at $n = 80, T = 0.8, k = 30$) indicate slight under-coverage in some situations, CPs are typically around or over the nominal 95% level. In general, Bayesian CPs are more stable.
- Similar to the trend shown for λ_1, Bayesian estimates forλ_2 in Table 7 are consistently higher than the MLEs in all scenarios. The greatest MSEs (e.g., 4.7433 for MLE at $n = 50, T = 0.5, k = 25$) are seen in CS III, suggesting lower precision under this censoring scheme. Though there are few outliers (e.g., Bayesian MSEs for CS II at $n = 80, T = 0.8, k = 55$ jump to 1.2300), larger samples ($n = 80$) typically result in lower MSEs (e.g., CS I MSEs drop from ∼1.1 to ∼0.14 for $T = 0.5, k = 30$). Similar to λ_1's sensitivity to censoring severity, higher censoring times (λ_1) frequently inflate MSEs (for example, the CS I MLE MSE increases from 1.1070 to 1.8512 for $k = 25$).
- As a result of more restrictive uncertainty estimation, the Bayesian ACI for λ_2 in Table 8 are smaller than MLE intervals (e.g., 0.3650 vs. 0.4137 for CS I at $n = 50, T = 0.5, k = 25$). Extreme narrowness, such as 0.1105 for the CS II Bayesian at $n = 80, T = 0.5, k = 30$, could be risky under-coverage, though. Although there are some minor variations (e.g., 0.9315 for CS II Bayesian at $n = 80, T = 0.5, k = 55$), the majority of CPs fall inside the nominal 95% range. For larger samples in particular, Bayesian CPs are considerably more stable.
- Each scenario in Table 9 shows that Bayesian estimates for λ_3 are consistently and significantly higher than the MLEs (e.g., 1.1640 vs. 0.8825 for CS I at $n = 50, T = 0.5, k = 25$). Bayesian MSEs remain higher, however, larger samples ($n = 80$) generally have lower MSEs (for example, in the CS I, the MLE and MSE decrease from 0.3712 to 0.1727 for $T = 0.5, k = 30$).
- Table 10 shows that there is more uncertainty in the Bayesian estimates for λ_3 because the Bayesian intervals are significantly wider than the MLE intervals (e.g., 0.4488 vs. 0.1950 for

CS I at $n = 50, T = 0.5, k = 25$). In contrast, patterns for λ_1 and λ_2 showed narrower Bayesian ranges. While Bayesian CPs are more stable, MLE intervals are good (e.g., 0.9309 for CS I at $n = 50,\ T = 0.5,\ k = 25$). The wider Bayesian intervals ensure better coverage.

Table 1. The MLEs and Bayesian estimates for α with the MSE in parentheses.

n	m	T	k	CS I		CS II		CS III	
				MLE	Bayes	MLE	Bayes	MLE	Bayes
50	40	0.5	25	1.5689	1.6051	1.5979	1.6199	1.8450	1.8641
				(0.0229)	(0.0489)	(0.3715)	(0.3764)	(0.2109)	(0.2072)
			35	1.9197	1.9361	1.9047	1.9219	1.9283	1.9404
				(0.0288)	(0.0379)	(0.0254)	(0.9560)	(0.0351)	(0.0380)
		0.8	25	1.5760	1.6055	1.5855	1.6136	1.8030	1.8294
				(0.0535)	(0.0639)	(0.0278)	(0.0547)	(0.0917)	(0.1032)
			35	1.9039	1.9212	1.9068	1.9229	1.9188	1.9361
				(0.0316)	(0.0374)	(0.0277)	(0.0343)	(0.0327)	(0.0417)
80	65	0.5	30	1.4174	1.4388	1.4078	1.4146	1.3498	1.3634
				(0.0059)	(0.0064)	(0.0066)	(0.0073)	(0.0099)	(0.0132)
			55	1.9439	1.9553	1.8726	1.8831	1.9304	1.9410
				(0.0165)	(0.0185)	(0.0163)	(0.0244)	(0.0252)	(0.0283)
		0.8	30	1.3984	1.4181	1.3509	1.3707	1.3477	1.3629
				(0.0119)	(0.0173)	(0.0112)	(0.0178)	(0.0104)	(0.0142)
			55	1.9380	1.9552	1.8765	1.8864	1.9297	1.9387
				(0.0154)	(0.0229)	(0.0160)	(0.0193)	(0.0249)	(0.0281)

Table 2. ACI and CP of MLE and Bayesian estimates for α with the CP in parentheses.

n	m	T	k	CS I		CS II		CS III	
				MLE	Bayes	MLE	Bayes	MLE	Bayes
50	40	0.5	25	0.0523	0.0614	0.0390	0.0418	0.0417	0.0360
				(0.9797)	(0.9733)	(0.9667)	(0.9702)	(0.9626)	(0.9803)
			35	0.0329	0.0313	0.0326	0.0318	0.0281	0.0260
				(0.9449)	(0.9537)	(0.9852)	(0.9344)	(0.9766)	(0.9781)
		0.8	25	0.0467	0.0510	0.0440	0.0493	0.0432	0.0500
				(0.9870)	(0.9432)	(0.9794)	(0.9374)	(0.9651)	(0.9333)
			35	0.0336	0.0345	0.0302	0.0298	0.0329	0.0328
				(0.9827)	(0.9617)	(0.9358)	(0.9530)	(0.9400)	(0.9621)
80	65	0.5	30	0.0497	0.0495	0.0231	0.0149	0.0290	0.0263
				(0.9615)	(0.9681)	(0.9304)	(0.9726)	(0.9345)	(0.9833)
			55	0.0283	0.0245	0.0233	0.0203	0.0252	0.0219
				(0.9511)	(0.9311)	(0.9799)	(0.9775)	(0.9514)	(0.9601)
		0.8	30	0.0370	0.0372	0.0353	0.0352	0.0309	0.0290
				(0.9794)	(0.9714)	(0.9385)	(0.9868)	(0.9851)	(0.9833)
			55	0.0357	0.0314	0.0233	0.0199	0.0244	0.0194
				(0.9894)	(0.9406)	(0.9729)	(0.9634)	(0.9358)	(0.9614)

Table 3. The MLEs and Bayesian estimates for β with the MSE in parentheses.

n	m	T	k	CS I		CS II		CS III	
				MLE	Bayes	MLE	Bayes	MLE	Bayes
50	40	0.5	25	7.0055	7.0055	7.4050	7.4050	6.0522	6.0522
				(1.9330)	(1.9330)	(2.4807)	(2.4807)	(1.0467)	(1.6407)
			35	6.3875	6.3875	6.5337	6.5337	6.4994	6.4994
				(0.8922)	(0.8922)	(0.9560)	(0.9560)	(1.1260)	(1.1260)
		0.8	25	7.0225	7.0225	7.5035	7.5035	6.3523	6.3523
				(2.0364)	(2.0364)	(2.8350)	(2.8350)	(1.9954)	(1.9954)
			35	6.4714	6.4714	6.5170	6.5170	6.5278	6.5278
				(1.0909)	(1.0909)	(0.9972)	(0.9972)	(0.9788)	(0.9788)
80	65	0.5	30	6.9726	6.9726	7.0732	7.0732	7.7363	7.7363
				(0.4216)	(0.4216)	(0.8122)	(0.8122)	(2.0254)	(2.0254)
			55	6.2549	6.2549	6.5093	6.5093	6.2310	6.2310
				(0.5404)	(0.5404)	(0.6337)	(0.6337)	(0.6719)	(0.6719)
		0.8	30	7.5227	7.5227	7.6571	7.6571	7.8342	7.8342
				(1.7134)	(1.7134)	(1.9015)	(1.9015)	(2.2364)	(2.2364)
			55	6.2892	6.2892	6.5011	6.5011	6.2377	6.2377
				(0.5319)	(0.5319)	(0.6618)	(0.6618)	(0.6066)	(0.6066)

Table 4. ACI and CP of MLE and Bayesian estimates for β with the CP in parentheses.

n	m	T	k	CS I		CS II		CS III	
				MLE	Bayes	MLE	Bayes	MLE	Bayes
50	40	0.5	25	0.0012	0.0011	0.0008	0.0007	0.0009	0.0008
				(0.9462)	(0.9634)	(0.9759)	(0.9744)	(0.9311)	(0.9545)
			35	0.0011	0.0012	0.0011	0.0010	0.0009	0.0008
				(0.9556)	(0.9845)	(0.9860)	(0.9897)	(0.9893)	(0.9727)
		0.8	25	0.0012	0.0011	0.0009	0.0008	0.0010	0.0009
				(0.9894)	(0.9390)	(0.9866)	(0.9734)	(0.9770)	(0.9781)
			35	0.0009	0.0010	0.0010	0.0011	0.0009	0.0008
				(0.9719)	(0.9724)	(0.9463)	(0.9637)	(0.9365)	(0.9388)
80	65	0.5	30	0.0005	0.0004	0.0006	0.0005	0.0007	0.0008
				(0.9712)	(0.9881)	(0.9328)	(0.9548)	(0.9599)	(0.9635)
			55	0.0008	0.0006	0.0009	0.0007	0.0008	0.0007
				(0.9565)	(0.9806)	(0.9872)	(0.9420)	(0.9496)	(0.9580)
		0.8	30	0.0008	0.0007	0.0005	0.0004	0.0006	0.0005
				(0.9857)	(0.9791)	(0.9884)	(0.9644)	(0.9860)	(0.9347)
			55	0.0009	0.0007	0.0005	0.0004	0.0010	0.0011
				(0.9426)	(0.9411)	(0.9777)	(0.9641)	(0.9386)	(0.9869)

Table 5. The MLEs and Bayesian estimates for λ_1 with the MSE in parentheses.

n	m	T	k	CS I		CS II		CS III	
				MLE	Bayes	MLE	Bayes	MLE	Bayes
50	40	0.5	25	2.0123	2.1482	2.2065	2.2891	3.1888	3.3014
				(1.2136)	(1.9306)	(0.9881)	(0.1603)	(5.7337)	(5.8452)
			35	2.7720	2.8355	2.7330	2.8154	2.8271	2.8701
				(0.6627)	(0.9988)	(0.5867)	(1.3848)	(0.7268)	(0.7885)
		0.8	25	2.0979	2.2117	2.1641	2.2978	2.7311	2.8130
				(4.8968)	(5.1810)	(1.8378)	(3.3556)	(2.0107)	(2.1936)
			35	2.7011	2.7603	2.7625	2.8113	2.7926	2.8625
				(0.7172)	(0.8339)	(0.6082)	(0.7315)	(0.6737)	(0.9178)
80	65	0.5	30	1.7020	1.8345	1.6810	1.7302	1.5198	7.7363
				(0.3297)	(0.4678)	(0.0886)	(0.1172)	(0.3894)	(0.4707)
			55	3.3114	3.3617	2.8050	2.8544	2.9552	3.0057
				(0.5642)	(0.6480)	(0.4057)	(0.6774)	(0.5124)	(0.7345)
		0.8	30	1.6029	1.6733	1.5530	1.6322	1.5049	1.5661
				(0.4862)	(0.6088)	(0.5206)	(0.7912)	(0.3993)	(0.6121)
			55	3.3077	3.4312	2.7846	2.8268	2.9407	2.9812
				(0.4982)	(1.9019)	(0.3904)	(0.4822)	(0.5310)	(0.7422)

Table 6. ACI and CP of MLE and Bayesian estimates for λ_1 with the CP in parentheses.

n	m	T	k	CS I		CS II		CS III	
				MLE	Bayes	MLE	Bayes	MLE	Bayes
50	40	0.5	25	0.4418	0.3401	0.3586	0.2458	0.3822	0.2801
				(0.9623)	(0.9363)	(0.9797)	(0.9525)	(0.9852)	(0.9647)
			35	0.3000	0.2046	0.3077	0.2382	0.2521	0.1700
				(0.9808)	(0.9544)	(0.9747)	(0.9571)	(0.9827)	(0.9860)
		0.8	25	0.3964	0.2877	0.4197	0.3116	0.3901	0.2739
				(0.9584)	(0.9480)	(0.9738)	(0.9344)	(0.9796)	(0.9630)
			35	0.2984	0.2036	0.2715	0.1888	0.3030	0.2044
				(0.9764)	(0.9719)	(0.9367)	(0.9579)	(0.9334)	(0.9817)
80	65	0.5	30	0.4040	0.2834	0.1988	0.1383	0.2370	0.1569
				(0.9422)	(0.9676)	(0.9770)	(0.9735)	(0.9356)	(0.9598)
			55	0.2949	0.1865	0.2245	0.1606	0.2345	0.1586
				(0.9326)	(0.9689)	(0.9627)	(0.9604)	(0.9594)	(0.9765)
		0.8	30	0.3076	0.2106	0.2859	0.2116	0.2526	0.1777
				(0.9342)	(0.9489)	(0.9771)	(0.9617)	(0.9434)	(0.9424)
			55	0.3850	0.3000	0.2187	0.1462	0.2249	0.1472
				(0.9384)	(0.9843)	(0.9623)	(0.9696)	(0.9324)	(0.9681)

Table 7. The MLEs and Bayesian estimates for λ_2 with the MSE in parentheses.

n	m	T	k	CS I		CS II		CS III	
				MLE	Bayes	MLE	Bayes	MLE	Bayes
50	40	0.5	25	1.8689	2.0455	1.9892	2.0879	2.6641	2.7370
				(1.1070)	(2.1235)	(0.6343)	(0.8366)	(4.7433)	(4.7369)
			35	2.7319	2.8170	2.6804	2.7918	2.7641	2.8159
				(0.6640)	(1.0505)	(0.5694)	(1.7683)	(0.6985)	(0.7599)
		0.8	25	1.8887	2.03333	2.0058	2.1572	2.5280	2.6114
				(1.8512)	(2.4695)	(1.6459)	(3.1118)	(2.4008)	(2.5856)
			35	2.6540	2.7358	2.7095	2.7881	2.7436	2.8353
				(0.6668)	(0.8321)	(0.6164)	(0.7932)	(0.7320)	(1.0222)
80	65	0.5	30	1.4863	1.5150	1.5679	1.5886	1.4063	1.4686
				(0.1434)	(0.1449)	(0.2991)	(0.3154)	(0.2487)	(0.3270)
			55	3.1232	3.1896	2.6098	2.6815	2.7770	2.8313
				(0.4835)	(0.5939)	(0.3828)	(1.2221)	(0.5097)	(0.6605)
		0.8	30	1.4607	1.5446	1.4367	1.5370	1.4223	1.5003
				(0.2832)	(0.3996)	(0.3821)	(0.6976)	(0.3144)	(0.5111)
			55	3.0943	3.2094	2.6162	2.6658	2.7565	2.8195
				(0.4408)	(1.2300)	(0.3497)	(0.4557)	(0.4896)	(0.9039)

Table 8. ACI and CP of MLE and Bayesian estimates for λ_2 with the CP in parentheses.

n	m	T	k	CS I		CS II		CS III	
				MLE	Bayes	MLE	Bayes	MLE	Bayes
50	40	0.5	25	0.4137	0.3650	0.3392	0.2565	0.3205	0.2358
				(0.9550)	(0.9814)	(0.9352)	(0.9789)	(0.9589)	(0.9378)
			35	0.2893	0.2190	0.2952	0.2516	0.2480	0.1679
				(0.9712)	(0.9409)	(0.9526)	(0.9774)	(0.9866)	(0.9635)
		0.8	25	0.3688	0.3226	0.3819	0.3116	0.3391	0.2431
				(0.9647)	(0.9682)	(0.9368)	(0.9700)	(0.9542)	(0.9445)
			35	0.2934	0.2197	0.2681	0.2101	0.3002	0.2336
				(0.9462)	(0.9554)	(0.9515)	(0.9571)	(0.9367)	(0.9885)
80	65	0.5	30	0.3529	0.2329	0.1868	0.1105	0.2148	0.1644
				(0.9521)	(0.9740)	(0.9622)	(0.9574)	(0.9395)	(0.9670)
			55	0.2755	0.1934	0.2134	0.1752	0.2201	0.1557
				(0.9721)	(0.9892)	(0.9443)	(0.9315)	(0.9622)	(0.9595)
		0.8	30	0.2759	0.2129	0.2695	0.2204	0.2373	0.1860
				(0.9801)	(0.9477)	(0.9374)	(0.9666)	(0.9347)	(0.9490)
			55	0.3510	0.2854	0.2054	0.1466	0.2152	0.1706
				(0.9386)	(0.9604)	(0.9417)	(0.9397)	(0.9618)	(0.9436)

Table 9. The MLEs and Bayesian estimates for λ_3 with the MSE in parentheses.

n	m	T	k	CS I		CS II		CS III	
				MLE	Bayes	MLE	Bayes	MLE	Bayes
50	40	0.5	25	0.8825	1.1640	0.9154	1.1352	1.4479	1.5879
				(0.3712)	(1.4363)	(0.8247)	(1.2691)	(2.2913)	(2.2890)
			35	1.2196	1.3604	1.2041	1.3807	1.2478	1.3697
				(0.1845)	(0.4135)	(0.1590)	(1.4132)	(0.2048)	(0.3413)
		0.8	25	0.9030	1.1427	0.9274	1.1876	1.0502	1.2285
				(0.3922)	(0.9935)	(0.4220)	(2.4600)	(0.3670)	(0.5935)
			35	1.1729	1.3351	1.2075	1.3525	1.2559	1.4306
				(0.1725)	(0.4651)	(0.1723)	(0.4373)	(0.2223)	(0.7548)
80	65	0.5	30	0.7150	0.9636	0.6139	0.6950	0.6545	1.4686
				(0.1727)	(0.5137)	(0.0903)	(0.1524)	(0.1945)	(0.3288)
			55	1.4115	1.5478	1.0837	1.1822	1.1646	1.2652
				(0.0856)	(0.2592)	(0.0994)	(0.4342)	(0.1208)	(0.2896)
		0.8	30	0.6785	0.8533	0.6750	0.8455	0.6731	0.8124
				(0.2090)	(0.4807)	(0.2967)	(0.7524)	(0.2581)	(0.5406)
			55	1.4154	1.6244	1.0843	1.1768	1.1526	1.2425
				(0.0913)	(1.1970)	(0.0883)	(0.2205)	(0.1226)	(0.2904)

Table 10. ACI and CP of MLE and Bayesian estimates for λ_3 with the CP in parentheses.

n	m	T	k	CS I		CS II		CS III	
				MLE	Bayes	MLE	Bayes	MLE	Bayes
50	40	0.5	25	0.1950	0.4488	0.1605	0.3551	0.1282	0.2207
				(0.9309)	(0.9427)	(0.9678)	(0.9335)	(0.9400)	(0.9417)
			35	0.1236	0.2338	0.1343	0.2874	0.1120	0.2042
				(0.9501)	(0.9751)	(0.9610)	(0.9663)	(0.9772)	(0.9393)
		0.8	25	0.1734	0.3896	0.1813	0.4089	0.1414	0.2956
				(0.9842)	(0.9818)	(0.9443)	(0.9584)	(0.9423)	(0.9733)
			35	0.1285	0.2666	0.1205	0.2393	0.1405	0.2874
				(0.9467)	(0.9463)	(0.9354)	(0.9346)	(0.9347)	(0.9815)
80	65	0.5	30	0.1744	0.4216	0.0806	0.1382	0.0977	0.1939
				(0.9554)	(0.9427)	(0.9734)	(0.9704)	(0.9400)	(0.9862)
			55	0.1276	0.2294	0.0858	0.1660	0.0919	0.1693
				(0.9493)	(0.9614)	(0.9313)	(0.9624)	(0.9734)	(0.9340)
		0.8	30	0.1304	0.2856	0.1224	0.2750	0.1069	0.2254
				(0.9761)	(0.9579)	(0.9551)	(0.9364)	(0.9356)	(0.9761)
			55	0.1619	0.3421	0.0849	0.1537	0.0871	0.1532
				(0.9882)	(0.9585)	(0.9643)	(0.9423)	(0.9836)	(0.9570)

6. Signal data analysis

To demonstrate the critical role of statistical inference in electrical engineering practice, particularly in radar signal processing and system optimization, we applied the methods developed earlier to analyze the arrival times of surveillance-radar returns measured near the detection threshold level. Using an AN/TPS-59(V)3 radar, data were experimentally measured on-site using an oscilloscope to monitor the received signal timings. The recorded signals, timed in milliseconds, fall into three categories:

- returns exceeding the detection threshold
- returns falling below the threshold
- ambiguous returns that either exceed the threshold but represent false alarms, or fall below the threshold despite originating from actual targets.

Several parameters, including the signal-to-noise ratio (SNR), probability of detection (Pd), and probability of false alarm (Pfa), affect the radar's performance concerning detection thresholds. Although the AN/TPS-59(V)3 does not have publicly available threshold graphs, its detection capabilities can be understood by applying general radar detection theory. With the red dashed line representing the detection threshold and the black line representing the received signal (target plus noise), the graph shown in Figure 5 displays a radar return signal over time. and the signal parts over the threshold, considered target detections, are represented by the shaded blue area.

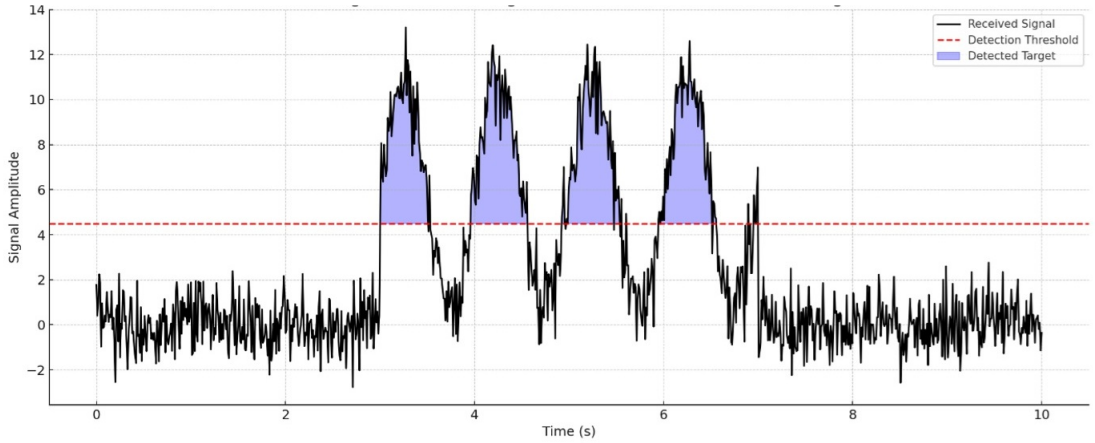

Figure 5. Radar signal detection: A signal above the threshold is considered a target.

The measurement experiment was carried out on two distinct occasions, designed to simulate different operational scenarios. During the initial experiment, the radar system was actively tracking a deliberately moving target. As the radar followed the target, it continuously logged the received signal power values, representing the strength of the signal reflected by the target. A threshold value of -79.850 dBm was established to discriminate between valid target detections and other signal types (e.g., noise). Signals with a power level stronger than this threshold were categorized as $U1$. $U1$ was defined as successful target detections; these comprised 34 out of the 41 readings, signifying a successful target detection rate of 80% under these moving target conditions. In contrast, signals with a power level weaker than -79.850 dBm were labeled $U3$, indicating the failure of the radar to detect the target. These missed detections accounted for 7 readings in total, suggesting potential limitations in detecting the target at certain points or under specific signal conditions.

The subsequent experiment involved a modification to the scenario, in which the target remained stationary. In this scenario, the primary objective was to characterize the power of the ambient signal, including background noise and potential interference, in the absence of movement of the target. In this specific environment, data points below the threshold of -79.850 dBm were assigned the label $U2$, which was defined as pure noise signals, reflecting the background radio frequency (RF) environment; these comprised many of the readings in the stationary target experiment, totaling 32 out of the 39 readings. In contrast, signals that exceeded -79.850 dBm, even though the target was stationary, were classified as $U3$. In this context, $U3$ was defined as representing false alarm scenarios in which the radar registered a signal above the detection threshold despite the absence of a legitimate moving target. These false alarms occurred in 7 out of the 39 readings, potentially caused by other sources of RF interference. The data set shown in Table 11 represents the received time for different signals in the three data sets.

Table 11. Extracted times of received signals for each of the three data sets.

$U1$	1.821	1.151	1.725	1.121	0.992	1.145	1.599	1.090	1.569	1.733	1.943
	1.911	1.734	1.741	1.097	0.846	1.008	1.387	1.463	1.631	1.423	1.358
	1.501	1.695	1.020	1.659	1.629	1.161	1.141	1.394	1.701	1.362	1.519
	1.407										
$U2$	1.406	1.292	1.323	1.187	1.099	0.894	1.583	1.404	1.924	1.596	1.489
	1.299	1.243	1.714	1.528	1.006	1.470	1.530	1.381	1.032	1.627	1.660
	1.278	1.52	1.522	1.513	1.112	1.507	1.267	2.027	0.963	1.179	
$U3$	1.242	1.758	1.386	1.495	1.481	1.787	1.302	1.695	1.426	1.560	1.359
	1.081	1.231	1.855								

We determine whether the PHW distribution with dependent competing risks can be used to model the data set under consideration. We apply goodness-of-fit analysis utilizing Watson U^2, Pearson's χ^2, Anderson-Darling, Cramér-von Mises, KS, and Kuiper. The distance and p-values (in brackets) for various tests are provided in Table 12 for the sets $U1$, $U2$, $U3$, and for the complete sample data. The findings demonstrate a decent match of the PHW distribution to the four data sets, with the p-values being relatively large and the distances being relatively small. Figure 6 shows the distances between the survival function for the PHW and the empirical distributions of the three data sets in Table 11, as well as the complete data set.

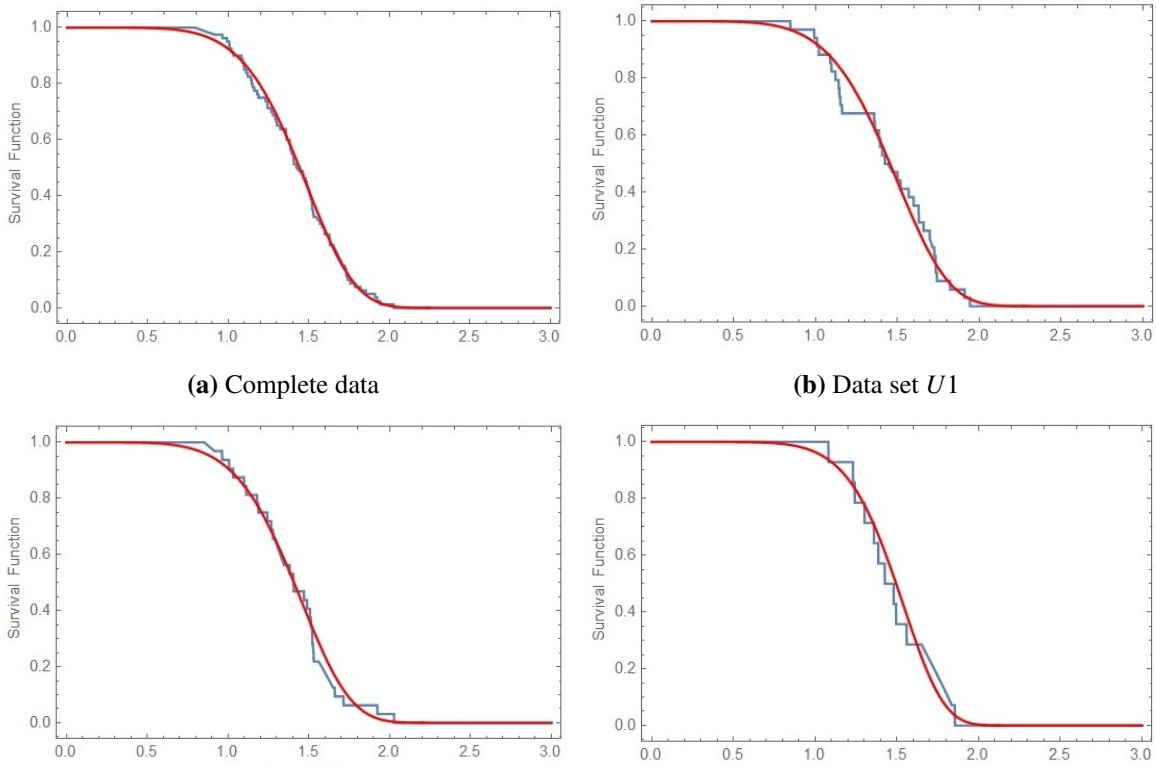

(a) Complete data

(b) Data set $U1$

(c) Data set $U2$

(d) Data set $U3$

Figure 6. Empirical and fitted survival functions for the data sets in Table 11.

Table 12. Measures of goodness-of-fit tests for signal data for different data sets.

	Complete data	Data set $U1$	Data set $U2$	Data set $U3$
Anderson-Darling	0.2664	0.5231	0.3696	0.3171
	(0.9610)	(0.7219)	(0.8774)	(0.9237)
Cramér-von Mises	0.0321	0.0808	0.0467	0.0523
	(0.9688)	(0.6871)	(0.8963)	(0.8621)
Kolmogorov-Smirnov	0.0548	0.1507	0.1087	0.1443
	(0.9589)	(0.3844)	(0.8054)	(0.8932)
Kuiper	0.0781	0.2099	0.1346	0.1815
	(0.9594)	(0.2192)	(0.8339)	(0.7953)
Pearson χ^2	6.7000	9.4118	4.0000	2.2857
	(0.5693)	(0.0937)	(0.4060)	(0.3189)
Watson U^2	0.0287	0.0808	0.0442	0.0493
	(0.9469)	(0.4102)	(0.7987)	(0.7641)

Three sets of GPHCS competing risk data are artificially obtained based on the real data provided in Table 11. These GPHCS data are provided in Table 13, where indicators 1–3 represent the three distinct sets of received radar data U_1, U_2, and U_3. Furthermore, for CS in Table 13, we used the notation $r = (2, 0^6)$, which means $r = (2, 0, 0, 0, 0, 0, 0)$.

Table 13. Generated GPHCS competing risks for the data sets in Table 11.

Scheme I: $n = 80,\ m = 60,\ k_1 = 45,\ T_1 = 0.5,\ r_1 = (0, 2^6, 0^{53})$											
$U1$	1.097	1.519	1.394	1.161	1.463	1.501	1.387	1.121	1.423	0.846	0.992
	1.145	1.151	1.141	1.090	1.362	1.407					
$U2$	1.507	0.894	0.963	1.006	1.381	1.267	1.278	1.323	1.187	1.243	1.520
	1.522	1.112	1.032	1.404	1.489	1.406	1.292	1.179	1.470		
$U3$	1.481	1.426	1.231	1.495	1.302	1.359	1.386	1.081			
Scheme II: $n = 80,\ m = 60,\ k_2 = 35,\ T_2 = 1.1,\ r_2 = (0^{32}, 2^6, 0^{22})$											
$U1$	1.020	1.145	1.090	1.387	1.121	1.161	0.846	0.992	1.358	1.141	1.151
	1.008	1.097	1.362								
$U2$	1.292	1.299	1.381	1.323	1.267	0.894	1.243	1.006	1.112	1.032	1.099
	1.278	1.187	0.963	1.179							
$U3$	1.081	1.242	1.386	1.231	1.302	1.359					
Scheme III: $n = 80,\ m = 60,\ k_3 = 50,\ T_3 = 1.35,\ r_3 = (0^{42}, 2^6, 0^{12})$											
$U1$	1.097	1.394	1.519	1.501	1.020	1.362	1.141	1.121	1.151	1.145	0.992
	1.008	1.090	0.846	1.358	1.463	1.423	1.407	1.387	1.161		
$U2$	1.489	1.507	1.299	1.179	1.112	0.894	1.522	1.406	1.292	1.470	1.032
	1.187	1.278	1.267	1.243	1.323	1.513	1.099	1.404	0.963	1.006	1.381
$U3$	1.359	1.495	1.386	1.242	1.426	1.302	1.081	1.231			

The hyperparameters in the gamma priors are assumed to be $a_1 = 10,\ a_2 = 15,\ a_3 = 140,\ a_4 = 200,\ a_5 = 0.0005,\ b_1 = 0.3,\ b_2 = 0.05,\ b_3 = 0.05,\ b_4 = 0.0001,\ b_5 = 18$ in the Bayesian technique.

Table 14 shows the point and interval estimates of the parameters under various censoring strategies when $T = 0.5$. Under the same censoring scheme, it is found that the estimation results of the five parameters from the MLE and Bayesian approaches are comparable. For λ_1, λ_3, and α, the Bayesian intervals are smaller than the ACIs. It seems that the ACI lengths for λ_2 are an exception, since some are smaller in Bayesian, while others are not. In addition, the Bayesian intervals are wider for β in some cases.

Table 14. Point and interval estimates for λ_1, λ_2, λ_3, α, and β.

	Censoring	MLE		Bayesian	
	Scheme	Point	Interval	SEL	Interval
	I	4.5076	{4.4893, 4.5260}[0.0367]	4.4971	{4.4833, 4.5111}[0.0278]
λ_1	II	4.4342	{4.4187, 4.4498}[0.0310]	4.4359	{4.4278, 4.4424}[0.0146]
	III	2.4182	{2.4150, 2.4214}[0.0065]	2.4164	{2.4147, 2.4190}[0.0042]
	I	5.0379	{5.0174, 5.0585} [0.0411]	5.0552	{5.0432, 5.0621}[0.0189]
λ_2	II	4.7510	{4.7343, 4.7676}[0.0333]	4.7458	{4.7341, 4.7690}[0.0349]
	III	2.6600	{2.6565, 2.6636}[0.0071]	2.6761	{2.6714, 2.6804}[0.0089]
	I	2.3864	{2.3767, 2.3961}[0.0194]	2.3845	{2.3799, 2.3876}[0.0077]
λ_3	II	1.9004	{1.8937, 1.9070}[0.0133]	1.9031	{1.8998, 1.9080}[0.0082]
	III	0.9673	{0.9660, 0.9686}[0.0026]	0.9680	{0.9671, 0.9686}[0.0015]
	I	1.8177	{1.8169, 1.8186}[0.0018]	1.8174	{1.8171, 1.8179}[0.0008]
α	II	1.7200	{1.7193, 1.7207}[0.0015]	1.7203	{1.7199, 1.7206}[0.0008]
	III	1.8058	{1.8055, 1.8061}[0.0007]	1.8055	{1.8053, 1.8057}[0.0003]
	I	8.4411	{8.4407, 8.4415}[0.0008]	8.4286	{8.4185, 8.4382}[0.0197]
β	II	8.2713	{8.2709, 8.2713}[0.0004]	8.2713	{8.2710, 8.2713}[0.0003]
	III	7.3167	{7.3166, 7.3168}[0.0002]	7.3176	{7.3101, 7.3313}[0.0212]

Since λ_3 is not equal to zero, our model makes sense, and 80 received signal times are entirely dependent. In actuality, if one is more concerned with the ease of estimation, they can select the outcomes from MLE. Bayesian estimates must be used if the estimation precision is more crucial. Figures 7 to 9 display the convergence of the estimated parameters $\lambda_1, \lambda_2, \lambda_3, \alpha$, and β for the three schemes, respectively, where N is the number of iterations performed using the MCMC approach. The values of every parameter sampled at each stage are shown in each trace plot. After some initial instability, the trace plots show comparatively stable patterns in a significant number of rounds. This suggests that the method has arrived at a stable sampling phase, since the MCMC chains probably have converged to a steady distribution.

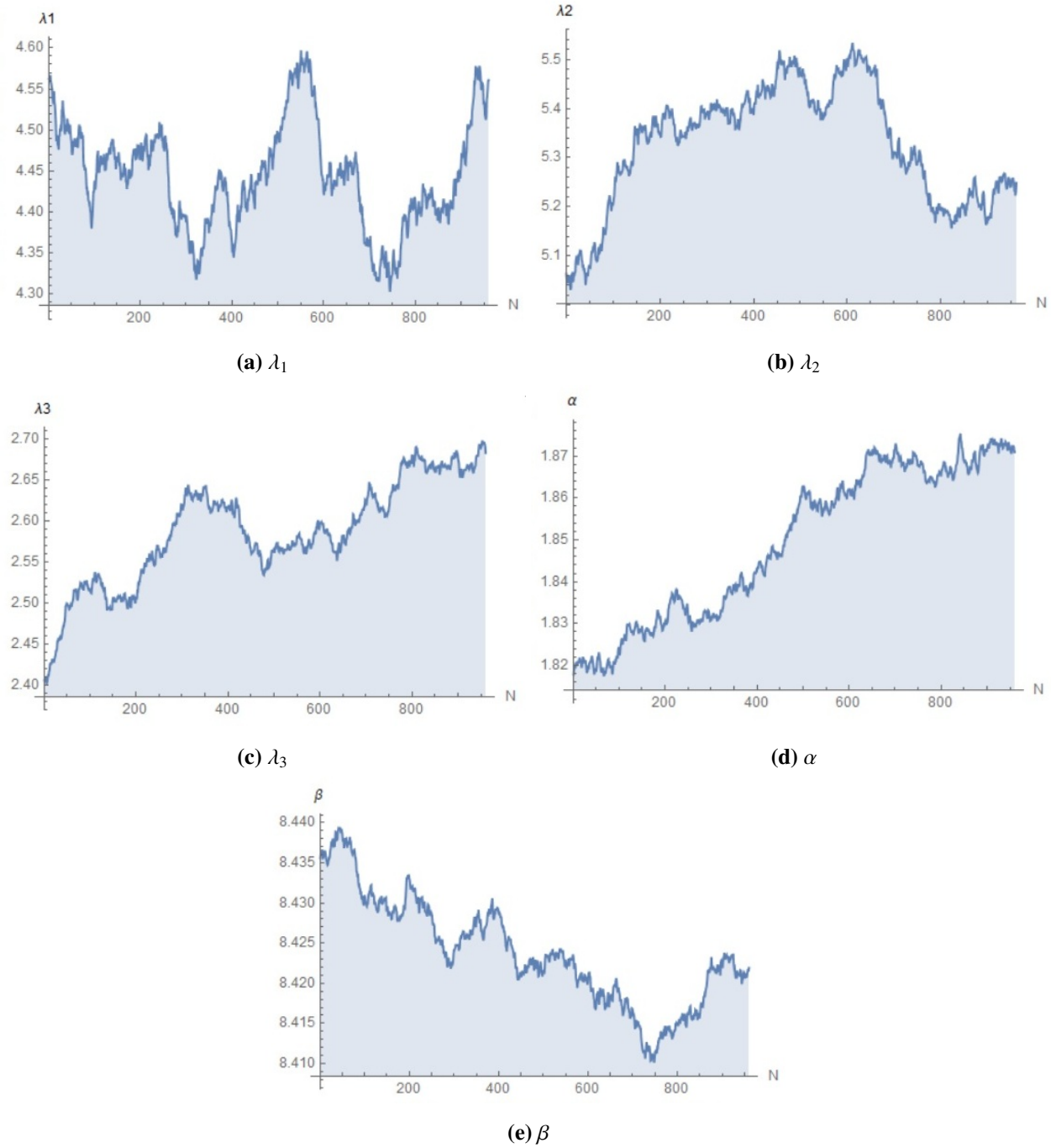

(a) λ_1 **(b)** λ_2

(c) λ_3 **(d)** α

(e) β

Figure 7. Convergence for the estimated parameters of $\lambda_1,\ \lambda_2,\ \lambda_3,\ \alpha$, and β for scheme I.

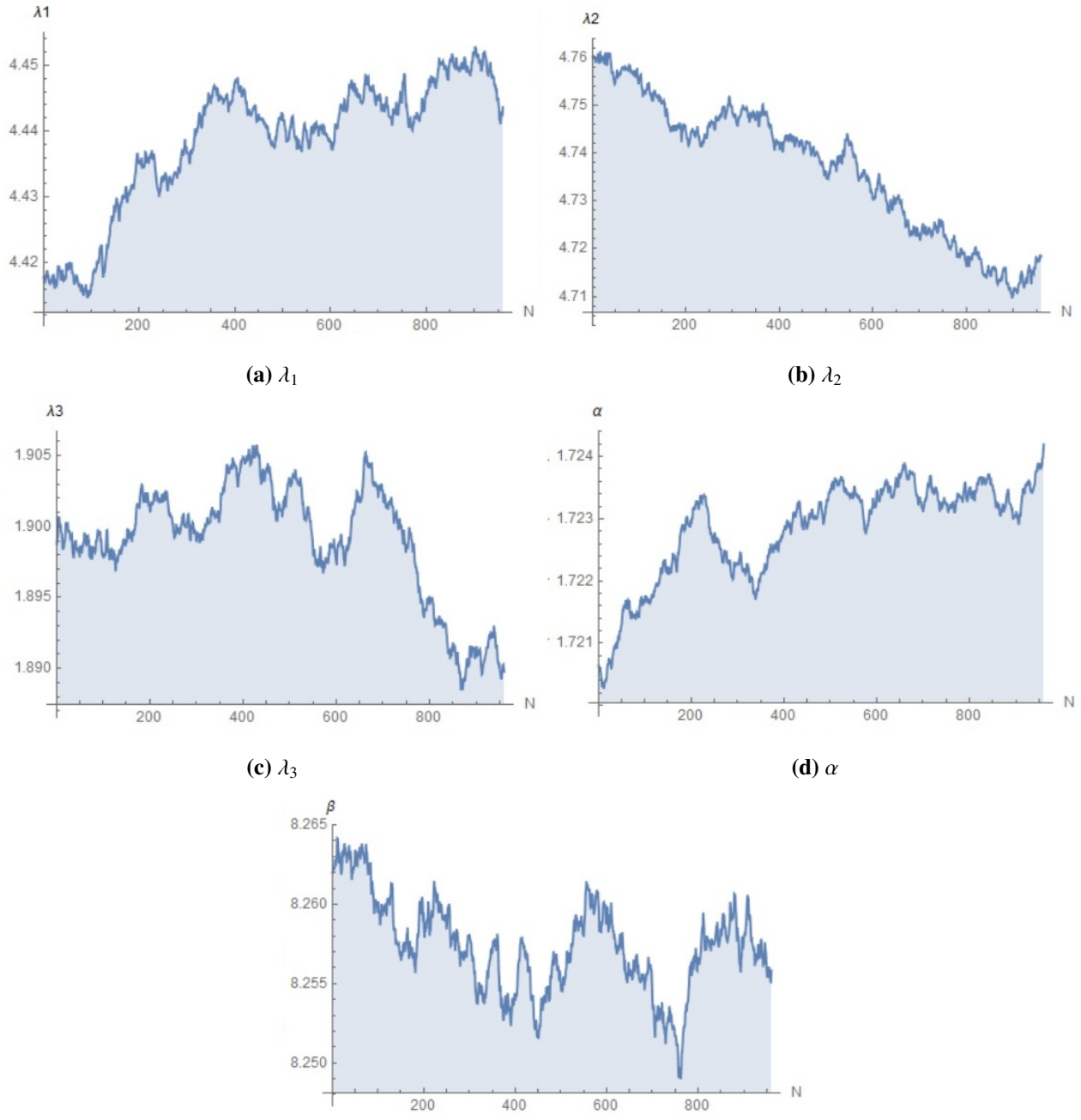

(a) λ_1 **(b)** λ_2 **(c)** λ_3 **(d)** α **(e)** β

Figure 8. Convergence for the estimated parameters of $\lambda_1,\ \lambda_2,\ \lambda_3,\ \alpha$, and β for scheme II.

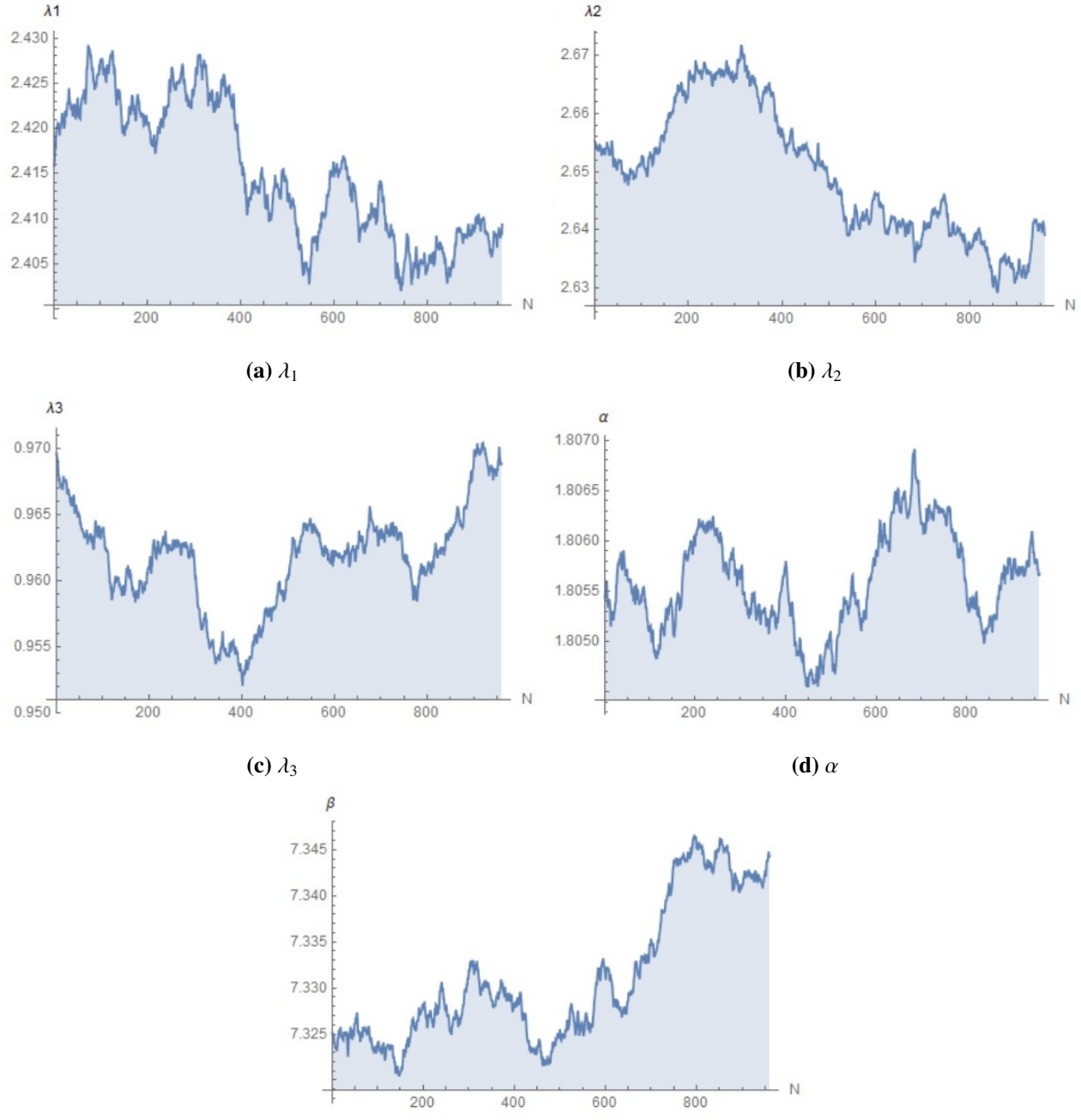

(a) λ_1 **(b)** λ_2

(c) λ_3 **(d)** α

(e) β

Figure 9. Convergence for the estimated parameters of $\lambda_1,\ \lambda_2,\ \lambda_3,\ \alpha$, and β for scheme III.

7. Conclusions

This study presents a comprehensive statistical framework for modeling radar signal detection performance under dependent competing risks using the PHW distribution. The GPHCS was employed due to its efficiency in balancing experimental duration and statistical inference quality. Both classical and Bayesian methods were used for point and interval estimation of the parameters. The effectiveness

of the proposed model was demonstrated through simulation and real-world signal data. The findings of this study suggest that although both MLE and Bayesian methods demonstrate strong reliability in terms of accuracy, the Bayesian approach outperforms in estimation efficiency, offering substantially narrower and more informative interval estimates. Several measures of goodness-of-fit tests were used, indicating the suitability of the proposed model to radar signal data. By coupling robust statistical theory with efficient numerical algorithms, the proposed framework offers a tractable yet powerful tool for analyzing dependent-risk lifetime data. It can be readily extended to other engineering and computational domains facing similar reliability challenges.

Future research may consider extending the model to accommodate more general baseline distributions or Bayesian frameworks that allow for dynamic prior updates. Another potential direction is the incorporation of covariate information or external stress variables using a frailty-based or semi-parametric extension of the PHW model. Finally, applying the proposed methodology to other engineering systems beyond radar, such as aerospace components, wireless sensors, or industrial devices, can further validate its practical robustness across disciplines.

Author contributions

Conceptualization, M. A., H. H. A., and D. R.; Methodology, M. A., H. H. A., and D. R.; Software: M. A., and A. E; validation, H. H. A., M. A.; Formal analysis: H. H. A., D. R., A. E. and M. A.; Investigation, A. E., M. A.; Resources: M. A, A. E.; Data curation: M. A, A. E.; Supervision, D. R, and H. H. A ; Writing—original draft, H. H. A., D. R, and M. A.; Writing—review and editing, H. H. A., D. R , M. A.; Funding acquisition, H. H. A.; All authors have read and agreed to the published version of the manuscript.

Use of Generative-AI tools declaration

The authors declare they have not used Artificial Intelligence (AI) tools in the creation of this article.

Funding

This work was supported by the Deanship of Scientific Research, Vice Presidency for Graduate Studies and Scientific Research, King Faisal University, Saudi Arabia [GRANT No. KFU252529].

Conflict of interest

The authors declare no conflicts of interest.

References

1. J. Fine, B. H. Lindqvist, Competing risks, *Lifetime Data Anal.*, **20** (2014), 159–160. https://doi.org/10.1007/s10985-014-9294-8
2. S. Liang, W. Gui, Parametric estimation and analysis of lifetime models with competing risks under middle-censored Data, *Appl. Sci.*, **15** (2025), 4288. https://doi.org/10.3390/app15084288

3. A. K. Mahto, C. Lodhi, Y. M. Tripathi, L. Wang, Inference for partially observed competing risks model for Kumaraswamy distribution under generalized progressive hybrid censoring, *J. Appl. Stat.*, **49** (2022), 2064–2092. https://doi.org/10.1080/02664763.2021.1889999
4. H. H. Ahmad, D. A. Ramadan, E. M. Almetwally, Tampered random variable analysis in step-stress testing: Modeling, inference, and applications, *Mathematics*, **12** (2024), 1248. https://doi.org/10.3390/math12081248
5. H. H. Ahmad, E. M. Almetwally, D. A. Ramadan, Competing risks in accelerated life testing: A study on step-stress models with tampered random variables, *Axioms*, **14** (2025), 32. https://doi.org/10.3390/axioms14010032
6. P. Chandra, H. K. Mandal, Y. M. Tripathi, L. Wang, Inference for depending competing risks from Marshall-Olkin bivariate Kies distribution under generalized progressive hybrid censoring, *J. Appl. Stat.*, **52** (2025), 936–965. https://doi.org/10.1080/02664763.2024.2405108
7. D. Samanta, D. Kundu, Bayesian inference of a dependent competing risk data, *J. Stat. Comput. Simul.*, **91** (2021), 3069–3086. https://doi.org/10.1080/00949655.2021.1917575
8. Y. Tian, W. Gui, Statistical inference of dependent competing risks from Marshall-Olkin bivariate Burr-XII distribution under complex censoring, *Commun. Stat. Simul. C.*, **53** (2024), 2988–3012. https://doi.org/10.1080/03610918.2022.2093373
9. F. A. Alqallaf, D. Kundu, A bivariate inverse generalized exponential distribution and its applications in dependent competing risks model, *Commun. Stat. Simul. C.*, **51** (2022), 7019–7036. https://doi.org/10.1080/03610918.2020.1821888
10. M. A. Richards, *Fundamentals of radar signal processing*, New York: Mcgraw-hill, 2005.
11. B. R. Mahafza, *Radar systems analysis and design using MATLAB*, New York: Chapman and Hall/CRC, 2005. https://doi.org/10.1201/9781420057072
12. M. G. Selim, G. G. Mabrouk, A. K. Elsherief, A. Youssef, Nonlinear Optimization Techniques for Radar Signal Enhancement, *2023 5th Novel Intelligent and Leading Emerging Sciences Conference (NILES)*, IEEE, 2023, 269–273, https://doi.org/10.1109/NILES59815.2023.10296549
13. Y. Zhang, J. Xi, S. Wang, D. Gao, G. Chang, Research on radar target recognition algorithms, *2023 3rd International Symposium on Artificial Intelligence and Intelligent Manufacturing (AIIM)*, IEEE, 2023, 30–33. https://doi.org/10.1109/AIIM60438.2023.10441184
14. N. Balakrishnan, Progressive censoring methodology: An appraisal, *Test*, **16** (2007), 211–259. https://doi.org/10.1007/s11749-007-0061-y
15. N. Balakrishnan, E. Cramer, *The art of progressive censoring: Applications to reliability and quality*, New York: Birkhäuser, 2014. https://doi.org/10.1007/978-0-8176-4807-7
16. A. Childs, B. Chandrasekar, N. Balakrishnan, Exact likelihood inference for an exponential parameter under progressive hybrid censoring schemes, In: *Statistical models and methods for biomedical and technical systems*, Boston: Birkhäuser, 2008. https://doi.org/10.1007/978-0-8176-4619-6_23
17. B. Epstein, Truncated life tests in the exponential case, *Ann. Soc. Polon. Math.*, **25** (1954), 555–564. 10.1214/aoms/117772872310.1214/aoms/1177728723

18. N. Ebrahimi, Estimating the parameters of an exponential distribution from hybrid life test, *J. Stat. Plan. Infer.*, **14** (1986), 255–261. https://doi.org/10.1016/0378-3758(86)90163-1
19. R. D. Gupta, D. Kundu, Hybrid censoring schemes with exponential failure distribution, *Commun. Stat. Theor. M.*, **27** (1998), 3065–3083. https://doi.org/10.1080/03610929808832273
20. C. T. Lin, Y. L. Huang, N. Balakrishnan, Exact Bayesian variable sampling plans for the exponential distribution based on Type-I and Type-II hybrid censored samples, *Commun. Stat. Simul. Comput.*, **37** (2008), 1101–1116. https://doi.org/10.1080/03610910801923869
21. J. Gorny, E. Cramer, Type-I hybrid censoring of multiple samples, *J. Comput. Appl. Math.*, **366** (2020), 112404. https://doi.org/10.1016/j.cam.2019.112404
22. D. Kundu, On hybrid censored Weibull distribution, *J. Stat. Plan. Infer.*, **137** (2007), 2127–2142. https://doi.org/10.1016/j.jspi.2006.06.043
23. D. Kundu, A. Joarder, Analysis of Type-II progressively hybrid censored data, *Comput. Stat. Data Anal.*, **50** (2006), 2509–2528. https://doi.org/10.1016/j.csda.2005.05.002
24. T. Sen, R. Bhattacharya, Y. M. Tripathi, B. Pradhan, Inference and optimum life testing plans based on type-II progressive hybrid censored generalized exponential data, *Commun. Stat. Simul. Comput.*, **49** (2020), 3254–3282. https://doi.org/10.1080/03610918.2018.1538456
25. Y. Cho, H. Sun, K. Lee, Exact likelihood inference for an exponential parameter under generalized progressive hybrid censoring scheme, *Stat. Methodol.*, **23** (2015), 18–34. https://doi.org/10.1016/j.stamet.2014.09.002
26. Y. Cho, H. Sun, K. Lee, Estimating the entropy of a Weibull distribution under generalized progressive hybrid censoring, *Entropy*, **17** (2015), 102–122. https://doi.org/10.3390/e17010102
27. A. Koley, D. Kundu, On generalized progressive hybrid censoring in presence of competing risks, *Metrika*, **80** (2017), 401–426. https://doi.org/10.1007/s00184-017-0611-6
28. S. Salem, O. E. Abo-Kasem, A. Hussien, On joint Type-II generalized progressive hybrid censoring scheme, *Comput. J. Math. Stat. Sci.*, **2** (2023), 123–158.
29. S. Dutta, S. Kayal, Estimation and prediction for Burr type III distribution based on unified progressive hybrid censoring scheme, *J. Appl. Stat.*, **51** (2024), 1–33. https://doi.org/10.1080/02664763.2022.2113865
30. L. Zhang, X. Chen, A. Khatab, Y. An, X. Feng, Joint optimization of selective maintenance and repairpersons assignment problem for mission-oriented systems operating under s-dependent competing risks, *Reliab. Eng. Syst. Safe.*, **242** (2024), 109796, https://doi.org/10.1016/j.ress.2023.109796
31. D. Kundu, A bivariate load-sharing model, *J. Appl. Stat.*, **52** (2025), 1446–1469. https://doi.org/10.1080/02664763.2024.2428267
32. N. Balakrishnan, D. Kundu, Hybrid censoring: Models, inferential results and applications, *Comput. Stat. Data Anal.*, **57** (2013), 166–209. https://doi.org/10.1016/j.csda.2012.03.025
33. G. Casella, R. Berger, *Statistical inference*, Oxford University, 2002.
34. J. F. Lawless, *Statistical models and methods for lifetime data*, John Wiley & Sons, 2002. https://doi.org/10.1002/9781118033005

35. N. Metropolis, A. W. Rosenbluth, M. N. Rosenbluth, A. H. Teller, E. Teller, Equation of state calculations by fast computing machines, *J. Chem. Phys.*, **21** (1953), 1087–1092. https://doi.org/10.1063/1.1699114

36. W. K. Hastings, Monte Carlo sampling methods using Markov chains and their applications, *Biometrika*, **57** (1970), 97–109.

37. I. Ntzoufras, *Bayesian modeling using WinBUGS*, John Wiley & Sons, 2011.

38. C. Robert, G. Casella, *Monte Carlo statistical methods*, New York: Springera, 2013. https://doi.org/10.1007/978-1-4757-4145-2

39. S. Chib, E. Greenberg, Understanding the Metropolis-Hastings algorithm, *Am. Stat.*, **49** (1995), 327–335. https://doi.org/10.1080/00031305.1995.10476177

Appendix 1

Proof. Given $U_1,\ U_2,\ U_3$ are three independent random variables, then

$$\begin{aligned} F_1(x) &= P(X_1 < x) = P(\min(U_1, U_3) < x) \\ &= 1 - P(U_1 > x)P(U_3 > x) \\ &= 1 - e^{-\lambda_1(\frac{x}{\alpha})^\beta} e^{-\lambda_3(\frac{x}{\alpha})^\beta} \\ &= 1 - e^{-(\lambda_1+\lambda_3)(\frac{x}{\alpha})^\beta}. \end{aligned}$$

Then $X_1 \sim PHW(\lambda_{13}, \alpha, \beta)$, where $\lambda_{13} = \lambda_1 + \lambda_3$. Similarly, it can be shown that $X_2 \sim PHW(\lambda_{23}, \alpha, \beta)$ and $\min(X_1,\ X_2) \sim PHW(\lambda_{123}, \alpha, \beta)$, where $\lambda_{23} = \lambda_2 + \lambda_3$ and $\lambda_{123} = \lambda_1 + \lambda_2 + \lambda_3$. □

Appendix 2

Proof.

$$\begin{aligned} S_{(X_1,X_2)}(x_1, x_2) &= P(\min(U_1, U_3) > x_1, \min(U_2, U_3) > x_2) \\ &= P(U_1 > x_1)P(U_2 > x_2)P(U_3 > \max(x_1, x_2)). \end{aligned}$$

We will then have three cases:

- If $x_1 < x_2$, then

$$\begin{aligned} S_{(X_1,X_2)}(x_1, x_2) &= P(U_1 > x_1)P(U_2 > x_2)P(U_3 > x_2) \\ &= e^{-\lambda_1(\frac{x_1}{\alpha})^\beta} e^{-\lambda_2(\frac{x_2}{\alpha})^\beta} e^{-\lambda_3(\frac{x_2}{\alpha})^\beta} \\ &= e^{-\lambda_1(\frac{x_1}{\alpha})^\beta} e^{-(\lambda_2+\lambda_3)(\frac{x_2}{\alpha})^\beta} \\ &= S(x_1; \lambda_1, \alpha, \beta) S(x_2; \lambda_{23}, \alpha, \beta). \end{aligned}$$

- If $x_1 > x_2$, then

$$\begin{aligned} S_{(X_1,X_2)}(x_1, x_2) &= P(U_1 > x_1)P(U_2 > x_2)P(U_3 > x_1) \\ &= e^{-\lambda_1(\frac{x_1}{\alpha})^\beta} e^{-\lambda_2(\frac{x_2}{\alpha})^\beta} e^{-\lambda_3(\frac{x_1}{\alpha})^\beta} \\ &= e^{-(\lambda_1+\lambda_3)(\frac{x_1}{\alpha})^\beta} e^{-\lambda_2(\frac{x_2}{\alpha})^\beta} \\ &= S(x_1; \lambda_{13}, \alpha, \beta) S(x_2; \lambda_2, \alpha, \beta). \end{aligned}$$

- If $x_1 = x_2 = x$, then

$$\begin{aligned} S_{(X_1,X_2)}(x_1,x_2) &= P(U_1 > x)P(U_2 > x)P(U_3 > x) \\ &= e^{-\lambda_1(\frac{x}{\alpha})^\beta} e^{-\lambda_2(\frac{x}{\alpha})^\beta} e^{-\lambda_3(\frac{x}{\alpha})^\beta} \\ &= e^{-(\lambda_1+\lambda_2+\lambda_3)(\frac{x}{\alpha})^\beta} \\ &= S(x;\lambda_{123},\alpha,\beta). \end{aligned}$$

□

Appendix 3

Proof. The joint PDF can be derived by simply calculating the partial derivatives of the joint survival function for the three different cases as:

- If $x_1 < x_2$, then

$$\begin{aligned} f_1(x_1,x_2) &= \frac{\partial^2}{\partial x_1 \partial x_2} S_{(X_1,X_2)}(x_1,x_2) \\ &= \frac{\partial^2}{\partial x_1 \partial x_2}\left[e^{-\lambda_1(\frac{x_1}{\alpha})^\beta} e^{-(\lambda_2+\lambda_3)(\frac{x_2}{\alpha})^\beta}\right] \\ &= \frac{\lambda_1\beta}{\alpha^\beta} x_1^{\beta-1} e^{-\lambda_1(\frac{x_1}{\alpha})^\beta} \frac{(\lambda_2+\lambda_3)\beta}{\alpha^\beta} x_2^{\beta-1} e^{-(\lambda_2+\lambda_3)(\frac{x_2}{\alpha})^\beta} \\ &= f(x_1;\lambda_1,\alpha,\beta) f(x_2;\lambda_{23},\alpha,\beta). \end{aligned}$$

- If $x_1 > x_2$, then

$$\begin{aligned} f_2(x_1,x_2) &= \frac{\partial^2}{\partial x_1 \partial x_2} S_{(X_1,X_2)}(x_1,x_2) \\ &= \frac{\partial^2}{\partial x_1 \partial x_2}\left[e^{-(\lambda_1+\lambda_3)(\frac{x_1}{\alpha})^\beta} e^{-\lambda_2(\frac{x_2}{\alpha})^\beta}\right] \\ &= \frac{(\lambda_1+\lambda_3)\beta}{\alpha^\beta} x_1^{\beta-1} e^{-(\lambda_1+\lambda_3)(\frac{x_1}{\alpha})^\beta} \frac{\lambda_2\beta}{\alpha^\beta} x_2^{\beta-1} e^{-\lambda_2(\frac{x_2}{\alpha})^\beta} \\ &= f(x_1;\lambda_{13},\alpha,\beta) f(x_2;\lambda_2,\alpha,\beta). \end{aligned}$$

- If $x_1 = x_2 = x$, then we can write

$$\int_0^\infty \int_0^{x_2} f_1(x_1,x_2)dx_1dx_2 + \int_0^\infty \int_0^{x_1} f_2(x_1,x_2)dx_2dx_1 + \int_0^\infty f_3(x)dx = 1,$$

where

$$\begin{aligned} \int_0^\infty \int_0^{x_2} f_1(x_1,x_2)dx_1dx_2 &= \int_0^\infty \int_0^{x_2} \frac{\lambda_1\beta}{\alpha^\beta} x_1^{\beta-1} e^{-\lambda_1(\frac{x_1}{\alpha})^\beta} \frac{\lambda_{23}\beta}{\alpha^\beta} x_2^{\beta-1} e^{-\lambda_{23}(\frac{x_2}{\alpha})^\beta} dx_1dx_2 \\ &= \int_0^\infty \left[1 - e^{-\lambda_1(\frac{x_2}{\alpha})^\beta}\right] \frac{\lambda_{23}\beta}{\alpha^\beta} x_2^{\beta-1} e^{-\lambda_{23}(\frac{x_2}{\alpha})^\beta} dx_2 \\ &= 1 - \frac{\lambda_{23}}{\lambda_{123}} = \frac{\lambda_1}{\lambda_{123}}, \end{aligned}$$

and

$$\begin{aligned}\int_0^{\infty}\int_0^{x_1} f_2(x_1,x_2)dx_2dx_1 &= \int_0^{\infty}\int_0^{x_1} \frac{\lambda_{13}\beta}{\alpha^{\beta}}x_1^{\beta-1}e^{-\lambda_{13}(\frac{x_1}{\alpha})^{\beta}}\frac{\lambda_2\beta}{\alpha^{\beta}}x_2^{\beta-1}e^{-\lambda_2(\frac{x_2}{\alpha})^{\beta}}dx_2dx_1\\ &= \int_0^{\infty}\left[1-e^{-\lambda_2(\frac{x_1}{\alpha})^{\beta}}\right]\frac{\lambda_{13}\beta}{\alpha^{\beta}}x_1^{\beta-1}e^{-\lambda_{13}(\frac{x_1}{\alpha})^{\beta}}dx_1\\ &= 1-\frac{\lambda_{13}}{\lambda_{123}} = \frac{\lambda_2}{\lambda_{123}}.\end{aligned}$$

Then

$$\int_0^{\infty} f_3(x)dx = 1-\frac{\lambda_1}{\lambda_{123}}-\frac{\lambda_2}{\lambda_{123}} = \frac{\lambda_3}{\lambda_{123}},$$

which leads to $f_3(x) = \frac{\lambda_3}{\lambda_{123}}f(x;\lambda_{123},\alpha,\beta)$.

□

AIMS Press